Beamforming Optimization for Active Intelligent Reflecting Surface-Aided SWIPT

Ying Gao, Qingqing Wu, *Senior Member, IEEE*, Guangchi Zhang, Wen Chen, *Senior Member, IEEE*, Derrick Wing Kwan Ng, *Fellow, IEEE*, and Marco Di Renzo, *Fellow, IEEE*

***Abstract*— *Active* intelligent reflecting surface (IRS) has been recently proposed to alleviate the product path loss attenuation inherent in the IRS-aided cascaded channel. In this paper, we study an active IRS-aided simultaneous wireless information and power transfer (SWIPT) system. Specifically, an active IRS is deployed to assist a multi-antenna access point (AP) to convey information and energy simultaneously to multiple single-antenna information users (IUs) and energy users (EUs). Two joint transmit and reflect beamforming optimization problems are investigated with different practical objectives. The first problem maximizes the weighted sum-power harvested by the EUs subject to individual signal-to-interference-plus-noise ratio (SINR) constraints at the IUs, while the second problem maximizes the weighted sum-rate of the IUs subject to individual energy harvesting (EH) constraints at the EUs. The optimization problems are non-convex and difficult to solve optimally. To tackle these two problems, we first rigorously prove that dedicated energy beams are not required for their corresponding semidefinite relaxation (SDR) reformulations and the SDR is tight for the first problem, thus greatly simplifying the AP precoding design. Then, by capitalizing on the techniques of alternating optimization (AO), SDR, and successive convex approximation (SCA), computationally efficient algorithms are developed to obtain suboptimal solutions of the resulting optimization problems. Simulation results demonstrate that, given the same total system power budget, significant performance gains in terms of operating range of wireless power transfer (WPT), total harvested energy, as well as achievable rate can be obtained by our proposed designs over benchmark schemes (especially the one adopting a passive IRS). Moreover, it is advisable to deploy an active IRS in the proximity of the users for the effective operation of WPT/SWIPT.**

***Index Terms*— Active intelligent reflecting surface (IRS), simultaneous wireless information and power transfer (SWIPT), beamforming optimization, radio frequency-based energy harvesting (EH).**

Manuscript received 29 March 2022; revised 8 June 2022; accepted 17 July 2022. Date of publication 3 August 2022; date of current version 9 January 2023. The work of Qingqing Wu was supported in part by FDCT under Grant 0119/2020/A3 and Grant SKL-IOTSC(UM)-2021-2023 and in part by GDST under Grant 2021A1515011900 and Grant 2020B1212030003. The work of Guangchi Zhang was supported in part by the Science and Technology Plan Project of Guangdong Province under Grant 2021A0505030015 and Grant 2020A050515010, in part by the Special Support Plan for High-Level Talents of Guangdong Province under Grant 2019TQ05X409, and in part by the Open Research Project Program of the State Key Laboratory of Internet of Things for Smart City (University of Macau) under Grant SKL-IoTSC(UM)-2021-2023/ORPF/A04/2022. The work of Wen Chen was supported in part by the National Key Project under Grant 2020YFB1807700 and Grant 2018YFB1801102, in part by the Shanghai Kewei under Grant 20JC1416502, and in part by NSFC under Grant 62071296. The work of Derrick Wing Kwan Ng was supported by the Australian Research Council's Discovery Project under Grant DP210102169. The work of Marco Di Renzo was supported in part by the European Commission through the H2020 ARIADNE Project under Grant 871464 and through the H2020 RISE-6G Project under Grant 101017011. The associate editor coordinating the review of this article and approving it for publication was D. Niyato. *(Corresponding author: Qingqing Wu.)*

Ying Gao and Qingqing Wu are with the State Key Laboratory of Internet of Things for Smart City, University of Macau, Taipa, Macao, China (e-mail: yinggao@um.edu.mo; qingqingwu@um.edu.mo).

Guangchi Zhang is with the School of Information Engineering, Guangdong University of Technology, Guangzhou 510006, China (e-mail: gczhang@gdut.edu.cn).

Wen Chen is with the Department of Electronic Engineering, Shanghai Jiao Tong University, Shanghai 201210, China (e-mail: wenchen@sjtu.edu.cn).

Derrick Wing Kwan Ng is with the School of Electrical Engineering and Telecommunications, University of New South Wales, Sydney, NSW 2052, Australia (e-mail: w.k.ng@unsw.edu.au).

Marco Di Renzo is with the Laboratoire des Signaux et Systèmes, CNRS, CentraleSupélec, Université Paris-Saclay, 91192 Gif-sur-Yvette, France (e-mail: marco.di-renzo@universite-paris-saclay.fr).

Color versions of one or more figures in this article are available at https://doi.org/10.1109/TWC.2022.3193845.

Digital Object Identifier 10.1109/TWC.2022.3193845

I. Introduction

With the increasing number and diversification of intelligent devices in Internet-of-Things (IoT) networks, emerging applications such as smart cities, mobile streaming media, and multisensory virtual reality become possible. One of the main challenges in the roll-out of reliable IoT is the energy limitation of battery-powered devices. Against this background, the dual use of radio frequency (RF) signals for enabling simultaneous wireless information and power transfer (SWIPT) has attracted intense interest [1]. However, energy users (EUs) and information users (IUs) typically operate with very different power sensitivity requirements (e.g., -10 dBm for EUs versus -60 dBm for IUs) [2]. As such, the operating range of wireless power transfer (WPT) is fundamentally limited by the severe path loss over long signal propagation distances, which restricts the performance of SWIPT systems. Although numerous multiple-input multiple-output (MIMO) technologies can considerably improve the efficiency of both WPT and wireless information transmission (WIT), their practical implementations are still hindered by the required exceedingly high energy consumption and hardware cost [3].

Recently, intelligent reflecting surface (IRS) or reconfigurable intelligent surface (RIS), comprised of a large number of passive metamaterial elements, has emerged as a cost- and energy-efficient solution to unlock the potential of future wireless networks [4]–[8]. Specifically, by smartly adapting

the phase shifts of all the IRS elements according to the time-varying environment, an IRS is capable of reconfiguring the wireless propagation channels for enhancing the desired signal strength and/or mitigating interference, thus improving the communication performance. It was firstly revealed in [5] that when the number of IRS elements, denoted by N, is large enough but finite, the receive signal power or the signal-to-noise ratio (SNR) gain scales with $\mathcal{O}(N^2)$ asymptotically. This pioneering result has then inspired major interests in studying the joint active and passive beamforming design for various system setups (see, e.g., [9]–[18]). While the works [5], [9]–[18] mainly focus on exploiting IRSs for effective WIT, the high passive beamforming gain promised by IRSs is also attractive for WPT [1], [4]. To reap this benefit, one line of research investigates IRS-aided wireless-powered communication networks (WPCNs), aiming at improving the communication performance by leveraging an IRS to assist WPT and WIT across different time slots [19]–[22]. On the other hand, another line of research focuses on exploiting the high passive beamforming gain to enlarge the rate-energy region of SWIPT systems offered by IRSs [23]–[28]. For example, the authors of [23] jointly optimized the transmit precoder at the access point (AP) and the phase shifts at the IRS to maximize the weighted sum-power of the EUs, while satisfying the minimum signal-to-interference-plus-noise ratio (SINR) requirements of the IUs. Inspired by [23], the authors of [24] studied the transmit power minimization subject to the individual quality-of-service (QoS) constraints at both the IUs and the EUs. Besides, the weighted sum-rate of all the IUs was maximized in [25], where the weighted sum-power harvested by all the EUs is ensured to be higher than a predefined value for QoS provisioning.

In spite of the appealing advantages of IRSs, the performance of passive IRS-aided systems may not offer a wide coverage extension because of the product path loss attenuation law, unless the number of IRS elements is very large [29]. Particularly, the end-to-end path loss of the transmitter-IRS-receiver link is generally significantly more severe than that of the unobstructed direct link, since the former is the product of the path losses of the transmitter-IRS and the IRS-receiver links. To circumvent this problem, one may need to install a large number of passive reflecting elements and/or to place the passive IRS in close vicinity of either the transmitter or the receiver, which, however, may not always be practically efficient or even feasible. As a remedy, the concept of *active* IRS has been proposed recently (see, e.g., [30], [31]) to alleviate the product path loss attenuation law. In particular, an active IRS is generally compromised of a number of active reflecting elements, each of which independently integrates a reflection-type amplifier, e.g., a tunnel diode, and thus cannot only alter the incident signals' phases, but also amplify them at the cost of additional low power consumption. Indeed, several papers in the field of metamaterials and communications have proved that an IRS can reflect the incident power with unitary power efficiency, for any angles of incidence and reflection, if local power gains and losses are present along the surface of the IRSs, see, e.g., [32]–[34]. The realization of these structures is more difficult than the conventional

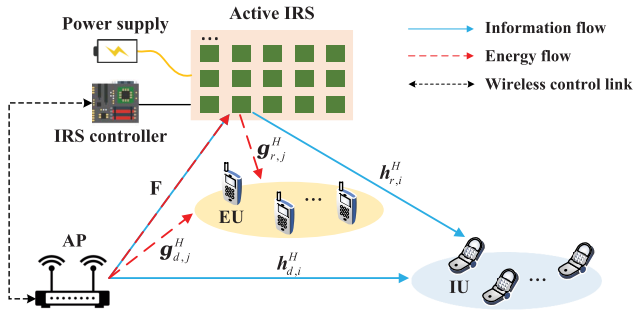

Fig. 1. An active IRS-aided SWIPT system.

design of locally-passive IRSs, but it usually results in better performance. The surfaces in [32]–[34] are usually globally passive, i.e., the reflected power is not greater than the incident power. In active IRSs, on the other hand, the reflected power is greater than the incident power. Both, however, assume that local power amplifications can be realized along the surface of the IRS. Recently, some innovative efforts have been devoted to beamforming optimization for active IRS-aided systems [30], [31], [35]–[38]. For instance, the authors of [30] studied the SNR maximization problem when introducing an active IRS into a single-input multiple-output (SIMO) system. The simulation results demonstrate that, given the same IRS power budget, an active IRS-aided system outperforms its passive counterpart. In [31], it is shown that an active IRS is capable of achieving noticeable capacity gains regardless of the strength of the direct link. Furthermore, the results in [35] indicate that, by optimizing the IRS placement, an active IRS has better performance than that of a passive IRS in some practical scenarios.

Although the above mentioned works have validated the superiority of adopting an active IRS over a passive IRS under some system setups, to our best knowledge, the potential performance gain of integrating an active IRS into SWIPT systems remains uninvestigated. Moreover, since the information signals for the IUs can be utilized at the EUs for energy harvesting (EH), some fundamental questions remain to be answered in active IRS-aided SWIPT systems. First, *are dedicated energy beams required to maximize the weighted sum-power of the EUs with the consideration of information transmission*? This question is motivated by the result in [23], which shows that dedicated energy beams are not required for a passive IRS-aided SWIPT system, generalizing the finding in [2] to the case with arbitrary user channels. For active IRS-assisted systems, however, the problem formulation of beamforming design is rather different due to the newly imposed amplification power constraint and the non-negligible IRS-amplified noise power. Thus, it is unknown whether the conclusions drawn in [23] still hold for active IRS-aided SWIPT systems. The second open question is: *is sending only information beams sufficient to satisfy the individual EH constraints at the EUs while maximizing the achievable weighted sum-rate of the IUs*? In other words, *can dedicated energy beams be removed or set to zero when solving the QoS-constrained weighted sum-rate maximization problem*? In [25], specially, the authors studied such a problem for a

passive IRS-aided SWIPT system, by simply assuming that there is no energy beamforming applied at the AP. Thus, the aforementioned fundamental issues remain unsolved.

Motivated by these considerations, we investigate an active IRS-aided SWIPT system where an active IRS is deployed to assist the information/power transfer from a multi-antenna AP to multiple single-antenna IUs and EUs, as shown in Fig. 1. The transmit precoder at the AP and the reflection-coefficient matrix at the IRS are jointly optimized by considering two different design criteria. In particular, the first problem maximizes the weighted sum-power harvested by the EUs subject to individual SINR constraints at the IUs, while the second problem maximizes the weighted sum-rate of the IUs subject to individual EH constraints at the EUs. The main contributions of this paper are summarized as follows.

- To obtain useful insights about active IRS-aided WPT systems, we first consider a special case of the weighted sum-power maximization problem where there exist no IUs and we apply the alternating optimization (AO), semidefinite relaxation (SDR), and successive convex approximation (SCA) techniques to obtain a suboptimal solution. Next, for the general case where the EUs and the IUs coexist, we rigorously prove that, despite the presence of a new amplification power constraint and non-negligible IRS-amplified noise power, dedicated energy beams are not required, which greatly simplifies the AP precoding design. Exploiting the obtained insight, we then propose a computationally efficient algorithm to solve the resulting problem suboptimally.
- For the weighted sum-rate maximization problem, we first unveil that dedicated energy beams are not needed for its SDR reformulation. Additionally, although the tightness of the SDR cannot be confirmed, a high-quality suboptimal solution for the original problem can be constructed from the optimal solution of the reformulated SDR problem. Building upon these insights, we consider the SDR reformulation with no dedicated energy beams to simplify the AP precoding design. Subsequently, we propose a computationally efficient suboptimal algorithm based on the AO and SCA techniques for the resulting problem and show how to approximately recover the transmit precoder if the obtained transmit beamforming matrices are not rank-one.
- Numerical results demonstrate that, by introducing an active IRS, the performance of SWIPT systems can be significantly enhanced in terms of operating range of WPT, total harvested energy, as well as achievable rate, as compared to passive IRS-aided SWIPT systems, under the assumption that the total system power budgets are the same. Furthermore, it is shown that the deployment of an active IRS close to the users is beneficial for WPT/SWIPT systems.

The remainder of this paper is organized as follows. Section II introduces the active IRS-aided SWIPT system model and presents the formulations of the weighted sum-power and sum-rate maximization problems. In Sections III and IV, we propose efficient algorithms for solving the two formulated problems, respectively. Numerical results are presented in Section V to evaluate the performance of the proposed algorithms. Finally, Section VI concludes the paper.

Notations: Scalars, vectors, and matrices are denoted in lower-case, boldface lower-case, and boldface upper-case letters, respectively. $\mathbb{C}^{x\times y}$ denotes the space of $x \times y$ complex-valued matrices. $\mathbb{H}^N$ represents the set of all N-dimensional complex Hermitian matrices. $\mathbb{E}(\cdot)$ denotes the statistical expectation. The distribution of a circularly symmetric complex Gaussian (CSCG) random vector with a mean vector $\boldsymbol{x}$ and a covariance matrix $\boldsymbol{\Sigma}$ is denoted by $\mathcal{CN}(\boldsymbol{x}, \boldsymbol{\Sigma})$. $\sim$ and $\triangleq$ stand for "distributed as" and "defined as", respectively. $\jmath$ denotes the imaginary unit, i.e., $\jmath^2 = 1$. The phase and real part of a complex number are denoted by $\arg(\cdot)$ and $\mathrm{Re}\{\cdot\}$, respectively. For a vector $\boldsymbol{a}$, $\|\boldsymbol{a}\|$ and $[\boldsymbol{a}]_n$ represent its Euclidean norm and n-th element, respectively. $\mathrm{diag}(\boldsymbol{a})$ denotes a diagonal matrix with each diagonal element being the corresponding element in $\boldsymbol{a}$. $\mathbf{I}_N$ is an identity matrix of size $N \times N$; $\mathbf{0}$ and $\mathbf{1}$ denote an all-zero matrix and an all-one matrix, respectively, with dimensions determined from the context. For a square matrix $\boldsymbol{S}$, $\mathrm{tr}(\boldsymbol{S})$ represents its trace; $\boldsymbol{S} \succeq \mathbf{0}$ indicates that $\boldsymbol{S}$ is positive semidefinite. For a matrix $\boldsymbol{A}$ of arbitrary size, $\|\boldsymbol{A}\|_F$, $\mathrm{rank}(\boldsymbol{A})$ and $[\boldsymbol{A}]_{i,j}$ denote its Frobenius norm, rank and (i,j)-th element, respectively. $(\cdot)^H$ corresponds to the conjugate transport of a vector or matrix. $\odot$ denotes the Hadamard product. For a set $\mathcal{K}$, $|\mathcal{K}|$ denotes its cardinality. $\mathcal{O}(\cdot)$ expresses the big-O notation.

II. System Model and Problem Formulation

A. System Model

As shown in Fig. 1, we consider an active IRS-aided SWIPT system, which comprises an AP with M antennas, an active IRS[1] with N reflecting elements, and two sets of single-antenna users, i.e., K_{I} IUs and K_{E} EUs, denoted by $\mathcal{K}_{\mathcal{I}} = \{1, \cdots, K_{\mathrm{I}}\}$ and $\mathcal{K}_{\mathcal{E}} = \{1, \cdots, K_{\mathrm{E}}\}$, respectively. In particular, the active IRS is supported by an external power supply and each of its elements cannot only alter the incident signals' phases, but also amplify the incident signals with an integrated reflection-type amplifier. Also, at the AP, we consider a linear transmit precoding for SWIPT with $\boldsymbol{w}_i \in \mathbb{C}^{M\times 1}$ and $\boldsymbol{v}_j \in \mathbb{C}^{M\times 1}$ denoting the beamforming vectors for IU i and EU j, respectively. Hence, the transmitted signal from the AP can be expressed as

$$\boldsymbol{x} = \sum_{i\in\mathcal{K}_{\mathcal{I}}} \boldsymbol{w}_i s_i^{\mathrm{I}} + \sum_{j\in\mathcal{K}_{\mathcal{E}}} \boldsymbol{v}_j s_j^{\mathrm{E}}, \tag{1}$$

where $s_i^{\mathrm{I}} \in \mathbb{C}$ and $s_j^{\mathrm{E}} \in \mathbb{C}$ are the information-bearing signal for IU i and the energy-carrying signal for EU j, respectively, satisfying $s_i^{\mathrm{I}} \sim \mathcal{CN}(0,1)$, $\forall i \in \mathcal{K}_{\mathcal{I}}$ and $\mathbb{E}\left(\left|s_j^{\mathrm{E}}\right|^2\right) = 1$, $\forall j \in \mathcal{K}_{\mathcal{E}}$ [2]. The two signals are assumed to be independent to each other. Let P_{A} denote the total transmit power budget of the AP. From (1), we have $\mathbb{E}\left(\boldsymbol{x}^H\boldsymbol{x}\right) = \sum_{i\in\mathcal{K}_{\mathcal{I}}} \|\boldsymbol{w}_i\|^2 + \sum_{j\in\mathcal{K}_{\mathcal{E}}} \|\boldsymbol{v}_j\|^2 \le P_{\mathrm{A}}$.

For characterizing the theoretical performance gain brought by an active IRS, we assume a quasi-static fading environment

[1]Note that the obtained results and the proposed algorithms can be extended to a *hybrid* IRS [39] by applying slight modifications.

and the channel state information (CSI)[2] of all channels is assumed to be acquired perfectly by the AP.[3] Let $\boldsymbol{h}_{d,i}^H \in \mathbb{C}^{1\times M}$ and $\boldsymbol{h}_{r,i}^H \in \mathbb{C}^{1\times N}$ denote the baseband equivalent channels from the AP to IU i and from the IRS to IU i, respectively. The corresponding channels for EU j are denoted by $\boldsymbol{g}_{d,j}^H \in \mathbb{C}^{1\times M}$ and $\boldsymbol{g}_{r,j}^H \in \mathbb{C}^{1\times N}$, respectively, and $\mathbf{F} \in \mathbb{C}^{N\times M}$ denotes the channel from the AP to the IRS. Let $\boldsymbol{\Theta} = \text{diag}\left(u_1, \cdots, u_N\right) \in \mathbb{C}^{N\times N}$ denote the reflection-coefficient matrix at the IRS. Particularly, u_n can be written as $u_n = \beta_n e^{j\theta_n}$, $n \in \mathcal{N} \triangleq \{1, \cdots, N\}$, where $\beta_n \geq 0$ and $\theta_n \in [0, 2\pi)$ represent the reflection amplitude and phase shift of the n-th IRS element, respectively. The signal received at IU i is then given by

$$\begin{aligned} y_i^{\text{I}} &= \underbrace{\boldsymbol{h}_{d,i}^H \boldsymbol{x}}_{\text{direct link}} + \underbrace{\boldsymbol{h}_{r,i}^H \boldsymbol{\Theta}\left(\mathbf{F}\boldsymbol{x} + \mathbf{z}\right)}_{\text{reflected link}} + n_i \\ &= \left(\boldsymbol{h}_{r,i}^H \boldsymbol{\Theta}\mathbf{F} + \boldsymbol{h}_{d,i}^H\right)\boldsymbol{x} + \boldsymbol{h}_{r,i}^H \boldsymbol{\Theta}\mathbf{z} + n_i, \quad i \in \mathcal{K}_{\mathcal{I}}, \end{aligned} \tag{2}$$

where $\mathbf{z} \sim \mathcal{CN}\left(\mathbf{0}, \sigma_z^2 \mathbf{I}_N\right)$ and $n_i \sim \mathcal{CN}\left(0, \sigma_i^2\right)$ denote the noise introduced by the active IRS [30] and the additive white Gaussian noise (AWGN) at IU i, respectively, with σ_z^2 and σ_i^2 being the corresponding noise variances. By assuming that the interference caused by the energy signals cannot be cancelled by the IUs, the SINR at IU i can be written as

$$\text{SINR}_i = \frac{\left|\boldsymbol{h}_i^H \boldsymbol{w}_i\right|^2}{\sum\limits_{k\in\mathcal{K}_{\mathcal{I}}\setminus\{i\}} \left|\boldsymbol{h}_i^H \boldsymbol{w}_k\right|^2 + \sum\limits_{j\in\mathcal{K}_{\mathcal{E}}} \left|\boldsymbol{h}_i^H \boldsymbol{v}_j\right|^2 + \sigma_z^2 \left\|\boldsymbol{h}_{r,i}^H \boldsymbol{\Theta}\right\|^2 + \sigma_i^2}, \quad i \in \mathcal{K}_{\mathcal{I}}, \tag{3}$$

where $\boldsymbol{h}_i^H \triangleq \boldsymbol{h}_{r,i}^H \boldsymbol{\Theta}\mathbf{F} + \boldsymbol{h}_{d,i}^H$ denotes the equivalent end-to-end channel from the AP to IU i. Accordingly, the achievable rate at IU i in bits/second/Hz (bps/Hz) is given by $R_i = \log_2\left(1 + \text{SINR}_i\right)$. On the other hand, the received RF power at EU j, denoted by Q_j, can be expressed as

$$Q_j = \sum_{i\in\mathcal{K}_{\mathcal{I}}} \left|\boldsymbol{g}_j^H \boldsymbol{w}_i\right|^2 + \sum_{m\in\mathcal{K}_{\mathcal{E}}} \left|\boldsymbol{g}_j^H \boldsymbol{v}_m\right|^2 + \sigma_z^2 \left\|\boldsymbol{g}_{r,j}^H \boldsymbol{\Theta}\right\|^2, \quad j \in \mathcal{K}_{\mathcal{E}}, \tag{4}$$

where $\boldsymbol{g}_j^H \triangleq \boldsymbol{g}_{r,j}^H \boldsymbol{\Theta}\mathbf{F} + \boldsymbol{g}_{d,j}^H$ denotes the equivalent end-to-end channel from the AP to EU j.[4]

Suppose that the active IRS is endowed with a maximum amplification power budget P_{I}. Then, we have $\sum_{i\in\mathcal{K}_{\mathcal{I}}} \left\|\boldsymbol{\Theta}\mathbf{F}\boldsymbol{w}_i\right\|^2 + \sum_{j\in\mathcal{K}_{\mathcal{E}}} \left\|\boldsymbol{\Theta}\mathbf{F}\boldsymbol{v}_j\right\|^2 + \sigma_z^2 \left\|\boldsymbol{\Theta}\right\|_F^2 \leq P_{\text{I}}$.

[2]If the IRS is equipped with active sensors, compressive sensing methods [40], [41] can be applied to estimate the channels of the AP-IRS and the IRS-user links, respectively; otherwise, the CSI of these links can be acquired by utilizing several existing methods, e.g., [42], [43].

[3]It is worth mentioning that, although this paper focuses on the case of perfect CSI, the results (i.e., Theorems 1 and 2) can be generalized to the case of imperfect CSI since the proof of Theorems 1 and 2 does not rely on the accuracy of the channel estimation. In general, it is of great interest to develop robust beamforming designs for the case of imperfect CSI. This, however, goes beyond the scope of this paper and is left for future work.

[4]For simplicity, we adopt a linear EH model which is widely used in existing works such as [19]–[21], [23]–[25]. The extension to the case with a non-linear EH model [27] is discussed in Remarks 3 and 5. Besides, the power of the antenna noise is ignored for EH while the noise power introduced by the active IRS is considered. This is because the former is generally a negligible constant, while the latter could be non-negligible, especially when the number of the reflecting elements, N, is sufficiently large.

B. Problem Formulation

Two joint transmit and reflect beamforming optimization problems are considered aiming at two different design criteria. First, we aim to maximize the weighted sum-power received at the EUs while satisfying individual SINR constraints at the IUs, given by γ_i, $i \in \mathcal{K}_{\mathcal{I}}$. From (4), the weighted sum-power received at the EUs can be written as

$$\sum_{j\in\mathcal{K}_{\mathcal{E}}} \alpha_j Q_j = \sum_{i\in\mathcal{K}_{\mathcal{I}}} \boldsymbol{w}_i^H \boldsymbol{S}\boldsymbol{w}_i + \sum_{j\in\mathcal{K}_{\mathcal{E}}} \boldsymbol{v}_j^H \boldsymbol{S}\boldsymbol{v}_j + \sum_{j\in\mathcal{K}_{\mathcal{E}}} \alpha_j \sigma_z^2 \left\|\boldsymbol{g}_{r,j}^H \boldsymbol{\Theta}\right\|^2, \tag{5}$$

where $\boldsymbol{S} \triangleq \sum_{j\in\mathcal{K}_{\mathcal{E}}} \alpha_j \boldsymbol{g}_j \boldsymbol{g}_j^H$ with $\alpha_j \geq 0$ denoting the given energy weight for EU j. Specifically, the larger the value of α_j, the higher priority given to EU j for EH. Accordingly, the problem of interest can be formulated as

$$\begin{aligned} (\text{P1}): \max_{\substack{\{\boldsymbol{w}_i\},\{\boldsymbol{v}_j\},\\ \boldsymbol{\Theta}}} \; & \sum_{i\in\mathcal{K}_{\mathcal{I}}} \boldsymbol{w}_i^H \boldsymbol{S}\boldsymbol{w}_i + \sum_{j\in\mathcal{K}_{\mathcal{E}}} \boldsymbol{v}_j^H \boldsymbol{S}\boldsymbol{v}_j + \sum_{j\in\mathcal{K}_{\mathcal{E}}} \alpha_j \sigma_z^2 \left\|\boldsymbol{g}_{r,j}^H \boldsymbol{\Theta}\right\|^2 && \text{(6a)} \\ \text{s.t. } & \text{SINR}_i \geq \gamma_i, \quad \forall i \in \mathcal{K}_{\mathcal{I}}, && \text{(6b)} \\ & \sum_{i\in\mathcal{K}_{\mathcal{I}}} \left\|\boldsymbol{w}_i\right\|^2 + \sum_{j\in\mathcal{K}_{\mathcal{E}}} \left\|\boldsymbol{v}_j\right\|^2 \leq P_{\text{A}}, && \text{(6c)} \\ & \sum_{i\in\mathcal{K}_{\mathcal{I}}} \left\|\boldsymbol{\Theta}\mathbf{F}\boldsymbol{w}_i\right\|^2 + \sum_{j\in\mathcal{K}_{\mathcal{E}}} \left\|\boldsymbol{\Theta}\mathbf{F}\boldsymbol{v}_j\right\|^2 + \sigma_z^2 \left\|\boldsymbol{\Theta}\right\|_F^2 \leq P_{\text{I}}. && \text{(6d)} \end{aligned}$$

Problem (P1) is applicable to the scenarios where the IUs have stringent SINR requirements (e.g., delay-limited transmission) while the EUs only require opportunistic EH.

In addition to (P1), we are also interested in maximizing the weighted sum-rate of the IUs subject to individual EH constraints at the EUs, given by E_j, $j \in \mathcal{K}_{\mathcal{E}}$. Let μ_i denote the weighting factor that controls the access priority of IU i. Then, we formulate the optimization problem as follows

$$\begin{aligned} (\text{P2}): \max_{\{\boldsymbol{w}_i\},\{\boldsymbol{v}_j\},\boldsymbol{\Theta}} \; & \sum_{i\in\mathcal{K}_{\mathcal{I}}} \mu_i \log_2\left(1 + \text{SINR}_i\right) && \text{(7a)} \\ \text{s.t. } & \sum_{i\in\mathcal{K}_{\mathcal{I}}} \left|\boldsymbol{g}_j^H \boldsymbol{w}_i\right|^2 + \sum_{m\in\mathcal{K}_{\mathcal{E}}} \left|\boldsymbol{g}_j^H \boldsymbol{v}_m\right|^2 + \sigma_z^2 \left\|\boldsymbol{g}_{r,j}^H \boldsymbol{\Theta}\right\|^2 \geq E_j, \quad \forall j \in \mathcal{K}_{\mathcal{E}}, && \text{(7b)} \\ & \text{(6c), (6d)}. && \text{(7c)} \end{aligned}$$

In contrast to (P1), (P2) applies to the scenarios where the EUs impose strict requirements on EH while the IUs have relaxed constraints for information transmission.

Since $\{\boldsymbol{w}_i\}$, $\{\boldsymbol{v}_j\}$, and $\boldsymbol{\Theta}$ are intricately coupled in the SINR_i of IU i given in (3), the received power Q_j of EU j given in (4), and the amplification power constraint given in (6d), optimization problems (P1) and (P2) are both non-convex, and are hence challenging to solve optimally. Moreover, for the considered active IRS-assisted SWIPT system, it remains unknown whether introducing dedicated energy beams $\{\boldsymbol{v}_j\}$ is necessary for achieving the optima of (P1) and (P2) in the presence of information beams $\{\boldsymbol{w}_i\}$.

III. Proposed Solution to Problem (P1)

In this section, we first consider and solve a special case of (P1) with no IUs to gain useful insights into active IRS-aided WPT systems. Then, we answer the question of whether the optimal solution to (P1) requires dedicated energy beams in the general case where the IUs and the EUs coexist. Finally, an efficient algorithm is proposed.

A. Special Case With No IUs

By setting $\boldsymbol{w}_i = \mathbf{0}$, $\gamma_i = 0$, $\forall i \in \mathcal{K}_\mathcal{I}$, (P1) is simplified to

$$\text{(P1-NoIUs)}: \max_{\{\boldsymbol{v}_j\},\boldsymbol{\Theta}} \sum_{j\in\mathcal{K}_\mathcal{E}} \boldsymbol{v}_j^H \boldsymbol{S}\boldsymbol{v}_j + \sum_{j\in\mathcal{K}_\mathcal{E}} \alpha_j \sigma_z^2 \left\|\boldsymbol{g}_{r,j}^H \boldsymbol{\Theta}\right\|^2 \tag{8a}$$

$$\text{s.t.} \sum_{j\in\mathcal{K}_\mathcal{E}} \|\boldsymbol{v}_j\|^2 \le P_\text{A}, \tag{8b}$$

$$\sum_{j\in\mathcal{K}_\mathcal{E}} \|\boldsymbol{\Theta}\mathbf{F}\boldsymbol{v}_j\|^2 + \sigma_z^2 \|\boldsymbol{\Theta}\|_F^2 \le P_\text{I}. \tag{8c}$$

The coupling between $\{\boldsymbol{v}_j\}$ and $\boldsymbol{\Theta}$ in both the objective function and constraint (8c) introduces non-convexities to (P1-NoIUs). To tackle this issue, we apply the AO method to iteratively optimize $\{\boldsymbol{v}_j\}$ and $\boldsymbol{\Theta}$ until convergence is reached, similar to [23] but with the exceptions given below.

1) Optimizing $\{\boldsymbol{v}_j\}$: For any given $\boldsymbol{\Theta}$, it was shown in [23] that, without constraint (8c), employing one dedicated energy beam is sufficient to achieve the optimality and the optimal energy precoder should be aligned to the dominant eigenvector of $\boldsymbol{S}$, denoted by $\boldsymbol{v}_{\boldsymbol{S}}$. However, with the newly introduced constraint (8c), whether employing one dedicated energy beam is sufficient to achieve the optimality is unknown, while aligning the energy precoder to $\boldsymbol{v}_{\boldsymbol{S}}$ may help to improve the objective value to a certain extent but yield a highly suboptimal solution. Therefore, the result in [23] is not directly applicable to the considered problem. In the following, we solve the subproblem with respect to $\{\boldsymbol{v}_j\}$ by applying the SDR technique [44] and answer the aforementioned question. Specifically, we define $\boldsymbol{W}_\text{E} = \sum_{j\in\mathcal{K}_\mathcal{E}} \boldsymbol{v}_j \boldsymbol{v}_j^H$, which needs to satisfy $\boldsymbol{W}_\text{E} \succeq \mathbf{0}$ and $\text{rank}\,(\boldsymbol{W}_\text{E}) \le \min(M, K_\text{E})$. By relaxing the rank constraint on $\boldsymbol{W}_\text{E}$, the subproblem can be recast as (with some constant terms ignored)

$$\max_{\boldsymbol{W}_\text{E}\in\mathbb{H}^M} \text{tr}\,(\boldsymbol{S}\boldsymbol{W}_\text{E}) \tag{9a}$$

$$\text{s.t. } \text{tr}\,(\boldsymbol{W}_\text{E}) \le P_\text{A},\ \text{tr}\,(\boldsymbol{C}\boldsymbol{W}_\text{E}) \le \bar{P}_\text{I},\quad \boldsymbol{W}_\text{E} \succeq \mathbf{0}, \tag{9b}$$

where $\boldsymbol{C} \triangleq \mathbf{F}^H \boldsymbol{\Theta}^H \boldsymbol{\Theta}\mathbf{F}$ and $\bar{P}_\text{I} \triangleq P_\text{I} - \sigma_z^2 \|\boldsymbol{\Theta}\|_F^2$. As problem (9) is a convex semidefinite program (SDP), it can be optimally solved by existing convex optimization solvers, e.g., CVX [45]. Regarding the rank of the obtained optimal solution, we have the following remark.

Remark 1: According to [46, Theorem 3.2], there exists an optimal solution $\boldsymbol{W}_\text{E}^*$ to problem (9) such that $(\text{rank}\,(\boldsymbol{W}_\text{E}^*))^2 \le 2$, where 2 corresponds to the number of linear constraints in (9). Moreover, if $P_\text{A} > 0$ and $\bar{P}_\text{I} > 0$, $\boldsymbol{W}_\text{E}^* = \mathbf{0}$ cannot be the optimal solution. Hence, an optimal solution that fulfills $\text{rank}\,(\boldsymbol{W}_\text{E}^*) = 1$ should exist for problem (9).

Although Remark 1 only indicates the existence of a rank-one optimal solution, the rank-reduction techniques in [46] can always be applied to construct a rank-one optimal solution from its non-rank-one optimal counterpart. Once obtained, $\boldsymbol{W}_\text{E}^*$ can be decomposed as $\boldsymbol{W}_\text{E}^* = \boldsymbol{v}_0^* (\boldsymbol{v}_0^*)^H$ via the Cholesky decomposition to recover the desired energy beamforming vector. Thus, we can choose to send only one energy beam to simplify the transmitter implementation by setting $\boldsymbol{v}_k = \boldsymbol{v}_0^*$ for any $k \in \mathcal{K}_\mathcal{E}$ and $\boldsymbol{v}_j = \mathbf{0}$, $\forall j \in \mathcal{K}_\mathcal{E}\backslash\{k\}$.

2) Optimizing $\boldsymbol{\Theta}$: For any given $\boldsymbol{v}_0^*$, $\boldsymbol{\Theta}$ can be optimized by solving (P1-NoIUs) with only the constraint in (8c). To facilitate the solution design, we define $\boldsymbol{u} = [u_1, \cdots, u_N]^H$, $\bar{\boldsymbol{u}} = [\boldsymbol{u}; 1]$, $\mathbf{G}_j = \left[\text{diag}\left(\boldsymbol{g}_{r,j}^H\right)\mathbf{F}; \boldsymbol{g}_{d,j}^H\right]$, $\mathbf{Z}_j = \text{diag}\left(\left[\boldsymbol{g}_{r,j}^H, 0\right]\right)\text{diag}\left(\left[\boldsymbol{g}_{r,j}; 0\right]\right)$, $\boldsymbol{\Phi} = \text{diag}\left(\left[\mathbf{F}\boldsymbol{v}_0^*; 0\right]\right) \times \left(\text{diag}\left(\left[\mathbf{F}\boldsymbol{v}_0^*; 0\right]\right)\right)^H$, and $\mathbf{P} = \text{diag}\left(\left[\mathbf{1}_{N\times 1}; 0\right]\right)$. Then, we have $\boldsymbol{g}_{r,j}^H \boldsymbol{\Theta}\mathbf{F} + \boldsymbol{g}_{d,j}^H = \bar{\boldsymbol{u}}^H \mathbf{G}_j$, $\left\|\boldsymbol{g}_{r,j}^H \boldsymbol{\Theta}\right\|^2 = \bar{\boldsymbol{u}}^H \mathbf{Z}_j \bar{\boldsymbol{u}}$, $\|\boldsymbol{\Theta}\mathbf{F}\boldsymbol{v}_0^*\|^2 = \bar{\boldsymbol{u}}^H \boldsymbol{\Phi}\bar{\boldsymbol{u}}$, and $\|\boldsymbol{\Theta}\|_F^2 = \bar{\boldsymbol{u}}^H \mathbf{P}\bar{\boldsymbol{u}}$. As a result, the subproblem is equivalent to

$$\max_{\bar{\boldsymbol{u}}} \sum_{j\in\mathcal{K}_\mathcal{E}} \alpha_j \left|\bar{\boldsymbol{u}}^H \mathbf{G}_j \boldsymbol{v}_0^*\right|^2 + \sum_{j\in\mathcal{K}_\mathcal{E}} \alpha_j \sigma_z^2 \bar{\boldsymbol{u}}^H \mathbf{Z}_j \bar{\boldsymbol{u}} \tag{10a}$$

$$\text{s.t. } \bar{\boldsymbol{u}}^H \boldsymbol{\Phi}\bar{\boldsymbol{u}} + \sigma_z^2 \bar{\boldsymbol{u}}^H \mathbf{P}\bar{\boldsymbol{u}} \le P_\text{I}, \tag{10b}$$

$$[\bar{\boldsymbol{u}}]_{N+1} = 1. \tag{10c}$$

Although maximizing a convex function results in a non-convex problem [45], the convexity of the objective function in (10a) allows us to apply the iterative SCA technique for solving problem (10) suboptimally. To begin with, the objective function can be written in a compact form as $\bar{\boldsymbol{u}}^H \mathbf{A}\bar{\boldsymbol{u}}$, where $\mathbf{A} = \sum_{j\in\mathcal{K}_\mathcal{E}} \alpha_j \left(\mathbf{G}_j \boldsymbol{v}_0^* (\boldsymbol{v}_0^*)^H \mathbf{G}_j^H + \sigma_z^2 \mathbf{Z}_j\right) \succeq 0$. Next, for a given local feasible point $\bar{\boldsymbol{u}}^{(l)}$ in the l-th iteration, the first-order Taylor expansion is a lower bound for $\bar{\boldsymbol{u}}^H \mathbf{A}\bar{\boldsymbol{u}}$ that can be expressed as

$$\bar{\boldsymbol{u}}^H \mathbf{A}\bar{\boldsymbol{u}} \ge 2\text{Re}\left\{\bar{\boldsymbol{u}}^H \mathbf{A}\bar{\boldsymbol{u}}^{(l)}\right\} - \left(\bar{\boldsymbol{u}}^{(l)}\right)^H \mathbf{A}\bar{\boldsymbol{u}}^{(l)} \triangleq \mathcal{G}^{(l)}(\bar{\boldsymbol{u}}). \tag{11}$$

By replacing the objective function in (10a) with $\mathcal{G}^{(l)}(\bar{\boldsymbol{u}})$, a suboptimal solution to (10) can be obtained by solving the following convex quadratically constrained quadratic program (QCQP):

$$\max_{\bar{\boldsymbol{u}}} \mathcal{G}^{(l)}(\bar{\boldsymbol{u}}) \tag{12a}$$

$$\text{s.t. (10b), (10c).} \tag{12b}$$

Remark 2: The value of the LHS of constraint (10b) is independent of the phase value of each element in $\bar{\boldsymbol{u}}$. Therefore, the optimal phase of u_n can be obtained in a closed-form expression given by $\theta_n^* = 0$ if $\left[\mathbf{A}\bar{\boldsymbol{u}}^{(l)}\right]_n = 0$ and $\theta_n^* = \arg\left(\left[\mathbf{A}\bar{\boldsymbol{u}}^{(l)}\right]_n\right)$ otherwise, $\forall n$. Then, only the real-number magnitudes of $\{u_n\}$ need to be optimized by solving problem (12) via existing convex optimization solvers, e.g., CVX [45]. This helps to reduce the simulation time.

3) Convergence and Complexity Analysis: As the objective value of (P1-NoIUs) is non-decreasing over the iterations and also upper-bounded by a finite value, the proposed algorithm is guaranteed to converge. Besides, the main computational burden stems from solving the SDP in (9) and the QCQP

in (12). Simply speaking, given a solution accuracy ε, problem (9) can be solved with a computational complexity[5] of $\mathcal{O}\left(M^{3.5}\log(\frac{1}{\varepsilon})\right)$, while the arithmetic cost[6] of solving problem (12) is less than $\mathcal{O}\left(N^{1.5}\ln\left(\frac{2(N+1)V}{\varepsilon}\right)\right)$, where V is a constant defined in [48] and $V > \varepsilon$. Thus, the total complexity of the proposed algorithm is about

$$\mathcal{O}\left[\Upsilon\left(M^{3.5}\log\left(\frac{1}{\varepsilon}\right)+N^{1.5}\ln\left(\frac{2(N+1)V}{\varepsilon}\right)\right)\right], \quad (13)$$

with Υ denoting the number of iterations required for convergence.

B. Are Dedicated Energy Beams Necessary?

Here, the general case where at least one IU coexists with $K_{\rm E}$ EUs is studied. In addition to the variables $\boldsymbol{C}$, $\bar{P}_{\rm I}$, and $\boldsymbol{W}_{\rm E}$ defined in the previous subsection, we define $\boldsymbol{W}_i = \boldsymbol{w}_i\boldsymbol{w}_i^H$, $\forall i \in \mathcal{K}_{\mathcal{I}}$. Then, it follows that $\boldsymbol{W}_i \succeq \boldsymbol{0}$ and $\mathrm{rank}\,(\boldsymbol{W}_i) \leq 1$, $\forall i \in \mathcal{K}_{\mathcal{I}}$. By dropping the rank constraints on $\boldsymbol{W}_{\rm E}$ and $\{\boldsymbol{W}_i\}$, the SDR reformulation of (P1) can be expressed as

$$\begin{aligned}
\text{(P1-SDR1)}: \max_{\substack{\{\boldsymbol{W}_i\in\mathbb{H}^M\},\\ \boldsymbol{W}_{\rm E}\in\mathbb{H}^M,\boldsymbol{\Theta}}} & \sum_{i\in\mathcal{K}_{\mathcal{I}}}\mathrm{tr}\,(\boldsymbol{S}\boldsymbol{W}_i)+\mathrm{tr}\,(\boldsymbol{S}\boldsymbol{W}_{\rm E}) \\
& +\sum_{j\in\mathcal{K}_{\mathcal{E}}}\alpha_j\sigma_z^2\left\|\boldsymbol{g}_{r,j}^H\boldsymbol{\Theta}\right\|^2 \quad (14a)\\
\text{s.t.}\ & \frac{\mathrm{tr}\left(\boldsymbol{h}_i\boldsymbol{h}_i^H\boldsymbol{W}_i\right)}{\gamma_i} \\
& -\sum_{k\in\mathcal{K}_{\mathcal{I}}\setminus\{i\}}\mathrm{tr}\left(\boldsymbol{h}_i\boldsymbol{h}_i^H\boldsymbol{W}_k\right) \\
& -\mathrm{tr}\left(\boldsymbol{h}_i\boldsymbol{h}_i^H\boldsymbol{W}_{\rm E}\right)-\bar{\sigma}_i^2\geq 0,\quad \forall i\in\mathcal{K}_{\mathcal{I}}, \quad (14b)\\
& \sum_{i\in\mathcal{K}_{\mathcal{I}}}\mathrm{tr}\,(\boldsymbol{W}_i)+\mathrm{tr}\,(\boldsymbol{W}_{\rm E})\leq P_{\rm A}, \quad (14c)\\
& \sum_{i\in\mathcal{K}_{\mathcal{I}}}\mathrm{tr}\,(\boldsymbol{C}\boldsymbol{W}_i)+\mathrm{tr}\,(\boldsymbol{C}\boldsymbol{W}_{\rm E})\leq \bar{P}_{\rm I}, \quad (14d)\\
& \boldsymbol{W}_i\succeq\boldsymbol{0},\quad \forall i\in\mathcal{K}_{\mathcal{I}},\ \boldsymbol{W}_{\rm E}\succeq\boldsymbol{0}, \quad (14e)
\end{aligned}$$

where $\bar{\sigma}_i^2 \triangleq \sigma_z^2\left\|\mathbf{h}_{r,i}^H\boldsymbol{\Theta}\right\|^2+\sigma_i^2$, $\forall i\in\mathcal{K}_{\mathcal{I}}$. If we remove constraint (14d), neglect the IRS-amplified noise power in (14a) and (14b), and set $\beta_n = 1$, $\forall n \in \mathcal{N}$, (P1-SDR1) is reduced to the same problem as in [23] for passive IRS-aided SWIPT systems. It was proved in [23, Proposition 1] that transmitting dedicated energy signals is not necessary. In particular, the proof of [23, Proposition 1] relies on the result in [2, Appendix A], which states that the optimal $\{\boldsymbol{W}_i\}$ and $\boldsymbol{W}_{\rm E}$ should all lie in the subspace spanned by one vector in the case that the optimal dual variables associated with the SINR constraints are all equal to zero. However, in the presence of constraint (14d), the above result cannot be proved to hold for (P1-SDR1) by following the same derivation as in [2, Appendix A]. Hence, for our considered active IRS-aided SWIPT system, we need to re-examine Proposition 1 in [23]. Fortunately, by exploiting the structure of (P1-SDR1), we have the following theorem.

Theorem 1: Assuming that (P1-SDR1) is feasible for $P_{\rm A} > 0$, $P_{\rm I} > 0$, and $\gamma_i > 0$, $\forall i \in \mathcal{K}_{\mathcal{I}}$, then there always exists an optimal solution to (P1-SDR1), denoted by $\{\{\boldsymbol{W}_i^*\},\boldsymbol{W}_{\rm E}^*,\boldsymbol{\Theta}^*\}$, satisfying $\boldsymbol{W}_{\rm E}^* = \boldsymbol{0}$ and $\mathrm{rank}\,(\boldsymbol{W}_i^*) = 1$, $\forall i \in \mathcal{K}_{\mathcal{I}}$.

Proof: Please refer to Appendix A. ∎

Remark 3: It is worth mentioning that (P1-SDR1) under a non-linear EH model [27] still has an optimal solution $\{\{\boldsymbol{W}_i^*\},\boldsymbol{W}_{\rm E}^*,\boldsymbol{\Theta}^*\}$ such that $\boldsymbol{W}_{\rm E}^* = \boldsymbol{0}$. The detailed proof is similar to that in Appendix A and is therefore omitted. However, whether $\mathrm{rank}\,(\boldsymbol{W}_i^*) = 1$, $\forall i \in \mathcal{K}_{\mathcal{I}}$ holds when $\boldsymbol{W}_{\rm E}^* = \boldsymbol{0}$ remains unknown and needs further investigation.

Remark 4: If the IUs have the capability of cancelling the interference due to the energy signals, the term $-\mathrm{tr}\left(\boldsymbol{h}_i\boldsymbol{h}_i^H\boldsymbol{W}_{\rm E}\right)$ should be removed in all the constraints in (14b). In this case, if $K_{\rm I} = 1$, the result presented in Theorem 1 can be similarly proved to hold. However, if $K_{\rm I} > 1$, $\boldsymbol{W}_{\rm E}^* \neq \boldsymbol{0}$ holds at least in some specific channel conditions. If the effective channels of the IUs and the EUs satisfy [2, Assumption 1], for example, then $\mathrm{rank}(\boldsymbol{W}_{\rm E}^*) \leq 1$ according to [2, Proposition 3.2].

Theorem 1 extends the result in [23] by showing that, even with the additional amplification power constraint in (14d) and the non-negligible IRS-amplified noise power in (14a) and (14b), the SDR is tight for (P1) and transmitting dedicated energy beams is not needed for achieving the optimal value of (P1). The intuitive explanation of this result is that transmitting dedicated energy beams would increase the interference power at the IUs while consuming power at the AP and at the IRS, and thus this should be avoided. By applying Theorem 1, the AP precoding design can be greatly simplified (especially when $K_{\rm E}$ is large) and (P1) is reduced to

$$\begin{aligned}
\max_{\{\boldsymbol{w}_i\},\boldsymbol{\Theta}} & \sum_{j\in\mathcal{K}_{\mathcal{E}}}\alpha_j\sum_{i\in\mathcal{K}_{\mathcal{I}}}\left|\left(\boldsymbol{g}_{r,j}^H\boldsymbol{\Theta}\mathbf{F}+\boldsymbol{g}_{d,j}^H\right)\boldsymbol{w}_i\right|^2 \\
& +\sum_{j\in\mathcal{K}_{\mathcal{E}}}\alpha_j\sigma_z^2\left\|\boldsymbol{g}_{r,j}^H\boldsymbol{\Theta}\right\|^2 \quad (15a)\\
\text{s.t.}\ & \frac{\left|\left(\boldsymbol{h}_{r,i}^H\boldsymbol{\Theta}\mathbf{F}+\boldsymbol{h}_{d,i}^H\right)\boldsymbol{w}_i\right|^2}{\sum\limits_{k\in\mathcal{K}_{\mathcal{I}}\setminus\{i\}}\left|\left(\boldsymbol{h}_{r,i}^H\boldsymbol{\Theta}\mathbf{F}+\boldsymbol{h}_{d,i}^H\right)\boldsymbol{w}_k\right|^2+\sigma_z^2\left\|\boldsymbol{h}_{r,i}^H\boldsymbol{\Theta}\right\|^2+\sigma_i^2} \\
& \geq\gamma_i,\quad \forall i\in\mathcal{K}_{\mathcal{I}}, \quad (15b)\\
& \sum_{i\in\mathcal{K}_{\mathcal{I}}}\left\|\boldsymbol{w}_i\right\|^2\leq P_{\rm A}, \quad (15c)\\
& \sum_{i\in\mathcal{K}_{\mathcal{I}}}\left\|\boldsymbol{\Theta}\mathbf{F}\boldsymbol{w}_i\right\|^2+\sigma_z^2\left\|\boldsymbol{\Theta}\right\|_F^2\leq P_{\rm I}. \quad (15d)
\end{aligned}$$

Although the problem at hand is simplified, it is still non-convex and difficult to solve, which motivates the development of the following algorithm.

[5]According to [47], the computational complexity of solving an SDP problem with m SDP constraints, each of which involves an n-dimensional positive semidefinite matrix, is given by $\mathcal{O}\left(\sqrt{n}\log\left(\frac{1}{\varepsilon}\right)\left(mn^3+m^2n^2+m^3\right)\right)$. For the SDP in (9), we have $m = 2$ and $n = M$.

[6]According to [48], the arithmetic cost for solving a QCQP problem with m variables and n quadratic constraints is given by $\mathcal{O}\left(\sqrt{m}\left(mn^2+n^3\right)\ln\left(\frac{2mV}{\varepsilon}\right)\right)$. For the QCQP in (12), we have $m = N+1$ and $n = 2$.

C. Proposed Algorithm for Problem (15)

Before solving problem (15), we first transform it into an equivalent but more tractable form. Similar to Section III-A, we define $\boldsymbol{u} = [u_1, \cdots, u_N]^H$, $\bar{\boldsymbol{u}} = [\boldsymbol{u}; 1]$, $\mathbf{G}_j = \left[\text{diag}\left(\boldsymbol{g}_{r,j}^H\right)\mathbf{F}; \boldsymbol{g}_{d,j}^H\right]$, $\mathbf{H}_i = \left[\text{diag}\left(\boldsymbol{h}_{r,i}^H\right)\mathbf{F}; \boldsymbol{h}_{d,i}^H\right]$, $\mathbf{Z}_j = \text{diag}\left(\left[\boldsymbol{g}_{r,j}^H, 0\right]\right)\text{diag}\left(\left[\boldsymbol{g}_{r,j}; 0\right]\right)$, $\mathbf{T}_i = \text{diag}\left(\left[\boldsymbol{h}_{r,i}^H, 0\right]\right)\text{diag}\left(\left[\boldsymbol{h}_{r,i}; 0\right]\right)$, $\mathbf{P} = \text{diag}\left(\left[\mathbf{1}_{N\times 1}; 0\right]\right)$, and $\mathbf{Q}_i = \left[\left(\mathbf{F}\boldsymbol{w}_i\boldsymbol{w}_i^H\mathbf{F}^H\right)\odot\mathbf{I}_N, \mathbf{0}; \mathbf{0}\right] \in \mathbb{C}^{(N+1)\times(N+1)}$. Then, we have $\boldsymbol{g}_{r,j}^H\boldsymbol{\Theta}\mathbf{F} + \boldsymbol{g}_{d,j}^H = \bar{\boldsymbol{u}}^H\mathbf{G}_j$, $\boldsymbol{h}_{r,i}^H\boldsymbol{\Theta}\mathbf{F} + \boldsymbol{h}_{d,i}^H = \bar{\boldsymbol{u}}^H\mathbf{H}_i$, $\left\|\boldsymbol{g}_{r,j}^H\boldsymbol{\Theta}\right\|^2 = \bar{\boldsymbol{u}}^H\mathbf{Z}_j\bar{\boldsymbol{u}}$, $\left\|\boldsymbol{h}_{r,i}^H\boldsymbol{\Theta}\right\|^2 = \bar{\boldsymbol{u}}^H\mathbf{T}_i\bar{\boldsymbol{u}}$, $\|\boldsymbol{\Theta}\|_F^2 = \bar{\boldsymbol{u}}^H\mathbf{P}\bar{\boldsymbol{u}}$, and $\|\boldsymbol{\Theta}\mathbf{F}\boldsymbol{w}_i\|^2 = \boldsymbol{u}^H\left(\left(\mathbf{F}\boldsymbol{w}_i\boldsymbol{w}_i^H\mathbf{F}^H\right)\odot\mathbf{I}_N\right)\boldsymbol{u} = \bar{\boldsymbol{u}}^H\mathbf{Q}_i\bar{\boldsymbol{u}}$. Therefore, problem (15) can be equivalently converted to

$$\max_{\{\boldsymbol{w}_i\},\bar{\boldsymbol{u}}} \sum_{j\in\mathcal{K}_\mathcal{E}}\alpha_j\sum_{i\in\mathcal{K}_\mathcal{I}}\left|\bar{\boldsymbol{u}}^H\mathbf{G}_j\boldsymbol{w}_i\right|^2 + \sum_{j\in\mathcal{K}_\mathcal{E}}\alpha_j\sigma_z^2\bar{\boldsymbol{u}}^H\mathbf{Z}_j\bar{\boldsymbol{u}} \tag{16a}$$

$$\text{s.t. } \left|\bar{\boldsymbol{u}}^H\mathbf{H}_i\boldsymbol{w}_i\right|^2 \geq \gamma_i\left(\sum_{k\in\mathcal{K}_\mathcal{I}\setminus\{i\}}\left|\bar{\boldsymbol{u}}^H\mathbf{H}_i\boldsymbol{w}_k\right|^2 + \sigma_z^2\bar{\boldsymbol{u}}^H\mathbf{T}_i\bar{\boldsymbol{u}} + \sigma_i^2\right), \quad \forall i\in\mathcal{K}_\mathcal{I}, \tag{16b}$$

$$\sum_{i\in\mathcal{K}_\mathcal{I}}\|\boldsymbol{w}_i\|^2 \leq P_\text{A}, \tag{16c}$$

$$\sum_{i\in\mathcal{K}_\mathcal{I}}\bar{\boldsymbol{u}}^H\mathbf{Q}_i\bar{\boldsymbol{u}} + \sigma_z^2\bar{\boldsymbol{u}}^H\mathbf{P}\bar{\boldsymbol{u}} \leq P_\text{I}, \tag{16d}$$

$$[\bar{\boldsymbol{u}}]_{N+1} = 1. \tag{16e}$$

Besides the matrices $\{\boldsymbol{W}_i\}$ defined in the previous subsection, we define another matrix $\boldsymbol{U}$, which is positive semidefinite and satisfies $\text{rank}(\boldsymbol{U}) \leq 1$. By utilizing the cyclic property of the trace operator and dropping the rank constraints on $\{\boldsymbol{W}_i\}$ and $\boldsymbol{U}$, the SDR reformulation of problem (16) is given by

$$\max_{\substack{\{\boldsymbol{W}_i\in\mathbb{H}^M\},\\ \boldsymbol{U}\in\mathbb{H}^{N+1}}} \sum_{j\in\mathcal{K}_\mathcal{E}}\alpha_j\sum_{i\in\mathcal{K}_\mathcal{I}}\text{tr}\left(\mathbf{G}_j\boldsymbol{W}_i\mathbf{G}_j^H\boldsymbol{U}\right) + \sum_{j\in\mathcal{K}_\mathcal{E}}\alpha_j\sigma_z^2\text{tr}\left(\mathbf{Z}_j\boldsymbol{U}\right) \tag{17a}$$

$$\text{s.t. } \text{tr}\left(\mathbf{H}_i\boldsymbol{W}_i\mathbf{H}_i^H\boldsymbol{U}\right) \geq \gamma_i\left(\sum_{k\in\mathcal{K}_\mathcal{I}\setminus\{i\}}\text{tr}\left(\mathbf{H}_i\boldsymbol{W}_k\mathbf{H}_i^H\boldsymbol{U}\right) + \sigma_z^2\text{tr}\left(\mathbf{T}_i\boldsymbol{U}\right) + \sigma_i^2\right), \quad \forall i\in\mathcal{K}_\mathcal{I}, \tag{17b}$$

$$\sum_{i\in\mathcal{K}_\mathcal{I}}\text{tr}\left(\boldsymbol{W}_i\right) \leq P_\text{A}, \tag{17c}$$

$$\sum_{i\in\mathcal{K}_\mathcal{I}}\text{tr}\left(\mathbf{Q}_i\boldsymbol{U}\right) + \sigma_z^2\text{tr}\left(\mathbf{P}\boldsymbol{U}\right) \leq P_\text{I}, \tag{17d}$$

$$[\boldsymbol{U}]_{N+1,N+1} = 1, \tag{17e}$$

$$\boldsymbol{W}_i \succeq \mathbf{0}, \quad \forall i\in\mathcal{K}_\mathcal{I},\ \boldsymbol{U}\succeq\mathbf{0}. \tag{17f}$$

However, problem (17) is still non-convex. Nevertheless, we note that, by fixing either $\{\boldsymbol{W}_i\}$ or $\boldsymbol{U}$, problem (17) is reduced to a standard convex SDP that can be optimally solved by existing convex optimization solvers, e.g., CVX [45]. Thus, this motivates us to utilize the AO method as in Section III-A to solve problem (17) by iteratively optimizing $\{\boldsymbol{W}_i\}$ and $\boldsymbol{U}$ until convergence is achieved.

Convergence and Complexity Analysis: The subproblem for updating $\{\boldsymbol{W}_i\}$ or $\boldsymbol{U}$ is optimally solved in each iteration, and thus the objective value of problem (17) is non-decreasing over the iterations. This, together with the fact that the optimal value of problem (17) is bounded from above, guarantees the convergence of the proposed algorithm. After the convergence of the AO algorithm, if the solution is not rank-one, we can obtain a rank-one solution for $\{\boldsymbol{W}_i\}$ by applying the rank reduction techniques in [46], and we can construct a rank-one solution for $\boldsymbol{U}$ by utilizing the Gaussian randomization method as in [49]. It is shown by simulation results in Section V that the objective value of problem (17) achieved by the solution constructed utilizing the Gaussian randomization method is almost the same as that when the AO algorithm converges. Regarding the computational complexity of the proposed algorithm, it is dominated by solving the two SDP subproblems. Similar to the analysis in Section III-A, the total computational complexity of the proposed algorithm is of the order of [47]

$$\mathcal{O}\left[\mathcal{L}\log\left(\frac{1}{\varepsilon}\right)\left(\left(M^{3.5}+N^{3.5}\right)K_\text{I} + \left(M^{2.5}+N^{2.5}\right)K_\text{I}^2 + \left(M^{0.5}+N^{0.5}\right)K_\text{I}^3\right)\right] \tag{18}$$

where ε is the solution accuracy and $\mathcal{L}$ denotes the number of iterations needed for convergence.

IV. Proposed Solution to Problem (P2)

In this section, we aim to solve (P2). First, we explore whether dedicated energy beams can be reasonably removed or set to zero when solving (P2). To facilitate the analysis, we start by introducing slack variables $\{\rho_i, \tau_i\}$, $i\in\mathcal{K}_\mathcal{I}$ such that

$$e^{\rho_i} = \sum_{k\in\mathcal{K}_\mathcal{I}}\left|\boldsymbol{h}_i^H\boldsymbol{w}_k\right|^2 + \sum_{j\in\mathcal{K}_\mathcal{E}}\left|\boldsymbol{h}_i^H\boldsymbol{v}_j\right|^2 + \bar{\sigma}_i^2, \quad \forall i\in\mathcal{K}_\mathcal{I}, \tag{19}$$

$$e^{\tau_i} = \sum_{k\in\mathcal{K}_\mathcal{I}\setminus\{i\}}\left|\boldsymbol{h}_i^H\boldsymbol{w}_k\right|^2 + \sum_{j\in\mathcal{K}_\mathcal{E}}\left|\boldsymbol{h}_i^H\boldsymbol{v}_j\right|^2 + \bar{\sigma}_i^2, \quad \forall i\in\mathcal{K}_\mathcal{I}, \tag{20}$$

where $\bar{\sigma}_i^2 \triangleq \sigma_z^2\left\|\mathbf{h}_{r,i}^H\boldsymbol{\Theta}\right\|^2 + \sigma_i^2$, $\forall i \in \mathcal{K}_\mathcal{I}$. Then, the objective function of (P2) can be equivalently written as $\sum_{i\in\mathcal{K}_\mathcal{I}}\mu_i\log_2 e^{(\rho_i-\tau_i)}$. Consequently, (P2) can be reformulated as follows

$$\text{(P2-Eqv)}: \max_{\substack{\{\boldsymbol{w}_i\},\{\boldsymbol{v}_j\},\\ \boldsymbol{\Theta},\{\rho_i,\tau_i\}}} \sum_{i\in\mathcal{K}_\mathcal{I}}\mu_i\log_2 e^{(\rho_i-\tau_i)} \tag{21a}$$

$$\text{s.t. } \sum_{k\in\mathcal{K}_\mathcal{I}}\left|\boldsymbol{h}_i^H\boldsymbol{w}_k\right|^2 + \sum_{j\in\mathcal{K}_\mathcal{E}}\left|\boldsymbol{h}_i^H\boldsymbol{v}_j\right|^2 + \bar{\sigma}_i^2 \geq e^{\rho_i}, \quad \forall i\in\mathcal{K}_\mathcal{I}, \tag{21b}$$

$$\sum_{k\in\mathcal{K}_\mathcal{I}\setminus\{i\}}\left|\boldsymbol{h}_i^H\boldsymbol{w}_k\right|^2 + \sum_{j\in\mathcal{K}_\mathcal{E}}\left|\boldsymbol{h}_i^H\boldsymbol{v}_j\right|^2$$

$$+\bar{\sigma}_i^2 \le e^{\tau_i}, \quad \forall i \in \mathcal{K}_\mathcal{I}, \tag{21c}$$

$$(7b), (6c), (6d). \tag{21d}$$

Note that the constraints in (21b) and (21c) are obtained by replacing the equality signs in (19) and (20) with inequality signs. At the optimal solution to (P2-Eqv), the constraints in (21b) and (21c) must be active, since otherwise the objective value can be further improved by increasing ρ_i (decreasing τ_i). Thus, (P2-Eqv) is equivalent to (P2). Recall that we defined $\boldsymbol{W}_i = \boldsymbol{w}_i\boldsymbol{w}_i^H$, $\forall i \in \mathcal{K}_\mathcal{I}$, $\boldsymbol{W}_\mathrm{E} = \sum_{j\in\mathcal{K}_\mathcal{E}} \boldsymbol{v}_j\boldsymbol{v}_j^H$, $\boldsymbol{C} = \mathbf{F}^H\boldsymbol{\Theta}^H\boldsymbol{\Theta}\mathbf{F}$, and $\bar{P}_\mathrm{I} = P_\mathrm{I} - \sigma_z^2\left\|\boldsymbol{\Theta}\right\|_F^2$ in the previous section. Then, the SDR reformulation of (P2-Eqv) can be expressed as

(P2-Eqv-SDR1) :

$$\max_{\substack{\{\boldsymbol{W}_i\in\mathbb{H}^M\},\\ \boldsymbol{W}_\mathrm{E}\in\mathbb{H}^M,\boldsymbol{\Theta},\{\rho_i,\tau_i\}}} \sum_{i\in\mathcal{K}_\mathcal{I}} \mu_i \log_2 e^{(\rho_i-\tau_i)} \tag{22a}$$

$$\text{s.t.} \sum_{k\in\mathcal{K}_\mathcal{I}} \mathrm{tr}\left(\boldsymbol{h}_i\boldsymbol{h}_i^H\boldsymbol{W}_k\right) + \mathrm{tr}\left(\boldsymbol{h}_i\boldsymbol{h}_i^H\boldsymbol{W}_\mathrm{E}\right) + \bar{\sigma}_i^2 \ge e^{\rho_i}, \quad \forall i \in \mathcal{K}_\mathcal{I}, \tag{22b}$$

$$\sum_{k\in\mathcal{K}_\mathcal{I}\setminus\{i\}} \mathrm{tr}\left(\boldsymbol{h}_i\boldsymbol{h}_i^H\boldsymbol{W}_k\right) + \mathrm{tr}\left(\boldsymbol{h}_i\boldsymbol{h}_i^H\boldsymbol{W}_\mathrm{E}\right) + \bar{\sigma}_i^2 \le e^{\tau_i}, \quad \forall i \in \mathcal{K}_\mathcal{I}, \tag{22c}$$

$$\sum_{i\in\mathcal{K}_\mathcal{I}} \mathrm{tr}\left(\boldsymbol{g}_j\boldsymbol{g}_j^H\boldsymbol{W}_i\right) + \mathrm{tr}\left(\boldsymbol{g}_j\boldsymbol{g}_j^H\boldsymbol{W}_\mathrm{E}\right) \ge \bar{E}_j, \quad \forall j \in \mathcal{K}_\mathcal{E}, \tag{22d}$$

$$\sum_{i\in\mathcal{K}_\mathcal{I}} \mathrm{tr}\left(\boldsymbol{W}_i\right) + \mathrm{tr}\left(\boldsymbol{W}_\mathrm{E}\right) \le P_\mathrm{A}, \tag{22e}$$

$$\sum_{i\in\mathcal{K}_\mathcal{I}} \mathrm{tr}\left(\boldsymbol{C}\boldsymbol{W}_i\right) + \mathrm{tr}\left(\boldsymbol{C}\boldsymbol{W}_\mathrm{E}\right) \le \bar{P}_\mathrm{I}, \tag{22f}$$

$$\boldsymbol{W}_i \succeq \mathbf{0}, \quad \forall i \in \mathcal{K}_\mathcal{I},\ \boldsymbol{W}_\mathrm{E} \succeq 0, \tag{22g}$$

where $\bar{E}_j \triangleq E_j - \sigma_z^2\left\|\boldsymbol{g}_{r,j}^H\boldsymbol{\Theta}\right\|^2$, $\forall j \in \mathcal{K}_\mathcal{E}$. Inspired by Theorem 1, we have the following theorem.

Theorem 2: Assuming that (P2-Eqv-SDR1) is feasible for $P_\mathrm{A} > 0$, $P_\mathrm{I} > 0$, and $E_j \ge 0$, $\forall j \in \mathcal{K}_\mathcal{E}$, then it always has an optimal solution $\{\{\boldsymbol{W}_i^*\}, \boldsymbol{W}_\mathrm{E}^*, \boldsymbol{\Theta}^*, \{\rho_i^*, \tau_i^*\}\}$ such that $\boldsymbol{W}_\mathrm{E}^* = \mathbf{0}$ and $\mathrm{rank}\,(\boldsymbol{W}_i^*) \le 1, \forall i \in \mathcal{K}_\mathcal{I}'$, where $\mathcal{K}_\mathcal{I}' \subseteq \mathcal{K}_\mathcal{I}$ and $|\mathcal{K}_\mathcal{I}'| \ge K_\mathrm{I} - 1$.

Proof: Please refer to Appendix B. ∎

Remark 5: For the case considering a non-linear EH model [27], the EH constraints in (22d) can be replaced by

$$\sum_{i\in\mathcal{K}_\mathcal{I}} \mathrm{tr}\left(\boldsymbol{g}_j\boldsymbol{g}_j^H\boldsymbol{W}_i\right) + \mathrm{tr}\left(\boldsymbol{g}_j\boldsymbol{g}_j^H\boldsymbol{W}_\mathrm{E}\right) \ge P_j(E_j) - \sigma_z^2\left\|\boldsymbol{g}_{r,j}^H\boldsymbol{\Theta}\right\|^2, \quad \forall j \in \mathcal{K}_\mathcal{E}, \tag{23}$$

where $P_j(E_j)$ is a function of E_j, whose value is known and fixed for a given E_j. It is not difficult to see that, by replacing the term $\bar{E}_j$ by $P_j(E_j) - \sigma_z^2\left\|\boldsymbol{g}_{r,j}^H\boldsymbol{\Theta}\right\|^2$ in Appendix B, we can immediately obtain the same result presented in Theorem 2 for the case adopting a non-linear EH model.

Remark 6: If the interference caused by the energy signals can be cancelled by the IUs, the term $\mathrm{tr}\left(\boldsymbol{h}_i\boldsymbol{h}_i^H\boldsymbol{W}_\mathrm{E}\right)$ should be removed in all the constraints in (22b) and (22c). If $K_\mathrm{I} = 1$, in this case, the result revealed in Theorem 2 can be similarly proved to hold. If $K_\mathrm{I} > 1$, however, the result may be different. Specifically, it is evident that (P2-Eqv-SDR1) without the term $\mathrm{tr}\left(\boldsymbol{h}_i\boldsymbol{h}_i^H\boldsymbol{W}_\mathrm{E}\right)$ always yields an equal or larger objective value than when it has the term $\mathrm{tr}\left(\boldsymbol{h}_i\boldsymbol{h}_i^H\boldsymbol{W}_\mathrm{E}\right)$. Meanwhile, (P2-Eqv-SDR1) with the term $\mathrm{tr}\left(\boldsymbol{h}_i\boldsymbol{h}_i^H\boldsymbol{W}_\mathrm{E}\right)$ does not need $\boldsymbol{W}_\mathrm{E}$ according to Theorem 2. Based on these facts, it can be concluded that a non-zero $\boldsymbol{W}_\mathrm{E}$ may help enhance the performance of (P2-Eqv-SDR1) without the term $\mathrm{tr}\left(\boldsymbol{h}_i\boldsymbol{h}_i^H\boldsymbol{W}_\mathrm{E}\right)$.

Since it is difficult to check if the SDR is tight for (P2-Eqv), it may not be concluded from Theorem 2 that dedicated energy signals are not needed for achieving the optimality of (P2-Eqv). Nevertheless, Theorem 2 indicates that the AP precoding design in (P2-Eqv-SDR1) can be simplified by setting $\boldsymbol{W}_\mathrm{E} = \mathbf{0}$ without any loss of optimality. Additionally, if the obtained optimal solution to (P2-Eqv-SDR1) does not satisfy the rank-one constraints on $\{\boldsymbol{W}_i\}$, we can always construct an alternative optimal solution that fulfills the condition $\mathrm{rank}\,(\boldsymbol{W}_i) \le 1$ for no less than $(K_\mathrm{I} - 1)$ $i \in \mathcal{K}_\mathcal{I}$, as presented in Appendix B. These considerations motivate us to focus on solving a simplified version of (P2-Eqv-SDR1), denoted by (P2-Eqv-SDR2) that is obtained by setting $\boldsymbol{W}_\mathrm{E} = \mathbf{0}$, instead of (P2-Eqv). To tackle (P2-Eqv-SDR2), we apply the AO method to decompose the problem into two subproblems which are then solved alternatingly until convergence is reached. The details are provided in the next subsections.

A. Transmit Beamforming Optimization

For any given $\boldsymbol{\Theta}$, the subproblem for optimizing $\{\boldsymbol{W}_i\}$ can be written as

$$\max_{\{\boldsymbol{W}_i\in\mathbb{H}^M\},\{\rho_i,\tau_i\}} \sum_{i\in\mathcal{K}_\mathcal{I}} \mu_i \log_2 e^{(\rho_i-\tau_i)} \tag{24a}$$

$$\text{s.t.} \sum_{k\in\mathcal{K}_\mathcal{I}} \mathrm{tr}\left(\boldsymbol{h}_i\boldsymbol{h}_i^H\boldsymbol{W}_k\right) + \bar{\sigma}_i^2 \ge e^{\rho_i}, \quad \forall i \in \mathcal{K}_\mathcal{I}, \tag{24b}$$

$$\sum_{k\in\mathcal{K}_\mathcal{I}\setminus\{i\}} \mathrm{tr}\left(\boldsymbol{h}_i\boldsymbol{h}_i^H\boldsymbol{W}_k\right) + \bar{\sigma}_i^2 \le e^{\tau_i}, \quad \forall i \in \mathcal{K}_\mathcal{I}, \tag{24c}$$

$$\sum_{i\in\mathcal{K}_\mathcal{I}} \mathrm{tr}\left(\boldsymbol{g}_j\boldsymbol{g}_j^H\boldsymbol{W}_i\right) \ge \bar{E}_j, \quad \forall j \in \mathcal{K}_\mathcal{E}, \tag{24d}$$

$$\sum_{i\in\mathcal{K}_\mathcal{I}} \mathrm{tr}\left(\boldsymbol{W}_i\right) \le P_\mathrm{A}, \tag{24e}$$

$$\sum_{i\in\mathcal{K}_\mathcal{I}} \mathrm{tr}\left(\boldsymbol{C}\boldsymbol{W}_i\right) \le \bar{P}_\mathrm{I}, \tag{24f}$$

$$\boldsymbol{W}_i \succeq \mathbf{0}, \quad \forall i \in \mathcal{K}_\mathcal{I}. \tag{24g}$$

However, constraint (24c) is non-convex since the right-hand-side (RHS) is convex with respect to τ_i, leading to the non-convexity of problem (24). To tackle this issue, the SCA technique is leveraged as in Section III-A. Specifically, we can replace the convex term e^{τ_i} in (24c) with its first-order Taylor expansion at a given local feasible point $\tau_i^{(t)}$. Then, the LHS

of constraint (24c) is upper-bounded by

$$\sum_{k\in\mathcal{K}_\mathcal{I}\setminus\{i\}} \mathrm{tr}\left(\boldsymbol{h}_i\boldsymbol{h}_i^H\boldsymbol{W}_k\right)+\bar{\sigma}_i^2 \le e^{\tau_i^{(t)}}\left(\tau_i-\tau_i^{(t)}+1\right), \quad \forall i\in\mathcal{K}_\mathcal{I}. \tag{25}$$

By replacing (24c) with (25), a suboptimal solution to problem (24) can be obtained by solving the following problem

$$\max_{\{\boldsymbol{W}_i\},\{\rho_i,\tau_i\}} \sum_{i\in\mathcal{K}_\mathcal{I}} \mu_i \log_2 e^{(\rho_i-\tau_i)} \tag{26a}$$

$$\text{s.t.} \quad (24\text{b}), (25), (24\text{d})-(24\text{g}). \tag{26b}$$

By direct inspection, problem (26) is a convex SDP and hence it can be optimally solved by using existing convex optimization solvers, e.g., CVX [45].

It is worth noting that, although problem (26) belongs to the class of separable SDPs and has an optimal solution that satisfies the condition $\sum_{i\in\mathcal{K}_\mathcal{I}}\left(\mathrm{rank}(\boldsymbol{W}_i)\right)^2 \le 2K_\mathrm{I}+K_\mathrm{E}+2$ according to [46, Theorem 3.2], this is not sufficient to prove that $\mathrm{rank}(\boldsymbol{W}_i)\le 1$, $\forall i\in\mathcal{K}_\mathcal{I}$ due to the arbitrariness of K_I and K_E. In addition, by using the duality principle and the Karush-Kuhn-Tucker (KKT) conditions, the optimal solution to problem (26) can be proved to satisfy $\mathrm{rank}(\boldsymbol{W}_i)\le 1$, $\forall i\in\mathcal{K}_\mathcal{I}$ provided that constraint (24e) is active at the optimal solution. The corresponding proof is similar to that of [50, Theorem 1] and it is thus omitted for brevity. Unfortunately, constraint (24e) is not necessarily active due to the existence of constraint (24f).

B. Reflect Beamforming Optimization

For any given $\{\boldsymbol{W}_i\}$, $\boldsymbol{\Theta}$ can be optimized by solving the following subproblem

$$\max_{\boldsymbol{\Theta},\{\rho_i,\tau_i\}} \sum_{i\in\mathcal{K}_\mathcal{I}} \mu_i \log_2 e^{(\rho_i-\tau_i)} \tag{27a}$$

$$\text{s.t.} \sum_{k\in\mathcal{K}_\mathcal{I}} \boldsymbol{h}_i^H\boldsymbol{W}_k\boldsymbol{h}_i+\sigma_z^2\left\|\boldsymbol{h}_{r,i}^H\boldsymbol{\Theta}\right\|^2+\sigma_i^2\ge e^{\rho_i}, \quad \forall i\in\mathcal{K}_\mathcal{I}, \tag{27b}$$

$$\sum_{k\in\mathcal{K}_\mathcal{I}\setminus\{i\}} \boldsymbol{h}_i^H\boldsymbol{W}_k\boldsymbol{h}_i+\sigma_z^2\left\|\boldsymbol{h}_{r,i}^H\boldsymbol{\Theta}\right\|^2+\sigma_i^2\le e^{\tau_i}, \quad \forall i\in\mathcal{K}_\mathcal{I}, \tag{27c}$$

$$\sum_{i\in\mathcal{K}_\mathcal{I}} \boldsymbol{g}_j^H\boldsymbol{W}_i\boldsymbol{g}_j+\sigma_z^2\left\|\boldsymbol{g}_{r,j}^H\boldsymbol{\Theta}\right\|^2\ge E_j, \quad \forall j\in\mathcal{K}_\mathcal{E}, \tag{27d}$$

$$\sum_{i\in\mathcal{K}_\mathcal{I}} \mathrm{tr}\left(\boldsymbol{\Theta}\mathbf{F}\boldsymbol{W}_i\mathbf{F}^H\boldsymbol{\Theta}^H\right)+\sigma_z^2\|\boldsymbol{\Theta}\|_F^2\le P_\mathrm{I}. \tag{27e}$$

To facilitate the solution of problem (27), we first transform it into a more tractable form. As in Section III-C, we define $\boldsymbol{u}=[u_1,\cdots,u_N]^H$, $\bar{\boldsymbol{u}}=[\boldsymbol{u};1]$, $\mathbf{H}_i=\left[\mathrm{diag}\left(\boldsymbol{h}_{r,i}^H\right)\mathbf{F};\boldsymbol{h}_{d,i}^H\right]$, $\mathbf{G}_j=\left[\mathrm{diag}\left(\boldsymbol{g}_{r,j}^H\right)\mathbf{F};\boldsymbol{g}_{d,j}^H\right]$, $\mathbf{T}_i=\mathrm{diag}\left(\left[\boldsymbol{h}_{r,i}^H,0\right]\right)\mathrm{diag}\left([\boldsymbol{h}_{r,i};0]\right)$, $\mathbf{Z}_j=\mathrm{diag}\left(\left[\boldsymbol{g}_{r,j}^H,0\right]\right)\mathrm{diag}\left(\left[\boldsymbol{g}_{r,j};0\right]\right)$, $\mathbf{P}=\mathrm{diag}\left([\mathbf{1}_{N\times1};0]\right)$, and $\mathbf{Q}_i=\left[\left(\mathbf{F}\boldsymbol{W}_i\mathbf{F}^H\right)\odot\mathbf{I}_N,\mathbf{0};\mathbf{0}\right]\in\mathbb{C}^{(N+1)\times(N+1)}$. Then, we have $\boldsymbol{h}_i^H=\bar{\boldsymbol{u}}^H\mathbf{H}_i$, $\boldsymbol{g}_j^H=\bar{\boldsymbol{u}}^H\mathbf{G}_j$, $\left\|\boldsymbol{h}_{r,i}^H\boldsymbol{\Theta}\right\|^2=\bar{\boldsymbol{u}}^H\mathbf{T}_i\bar{\boldsymbol{u}}$, $\left\|\boldsymbol{g}_{r,j}^H\boldsymbol{\Theta}\right\|^2=\bar{\boldsymbol{u}}^H\mathbf{Z}_j\bar{\boldsymbol{u}}$, $\|\boldsymbol{\Theta}\|_F^2=\bar{\boldsymbol{u}}^H\mathbf{P}\bar{\boldsymbol{u}}$, and $\mathrm{tr}\left(\boldsymbol{\Theta}\mathbf{F}\boldsymbol{W}_i\mathbf{F}^H\boldsymbol{\Theta}^H\right)=\boldsymbol{u}^H\left(\left(\mathbf{F}\boldsymbol{W}_i\mathbf{F}^H\right)\odot\mathbf{I}_N\right)\boldsymbol{u}=\bar{\boldsymbol{u}}^H\mathbf{Q}_i\bar{\boldsymbol{u}}$. Accordingly, problem (27) can be equivalently written as

$$\max_{\bar{\boldsymbol{u}},\{\rho_i,\tau_i\}} \sum_{i\in\mathcal{K}_\mathcal{I}} \mu_i \log_2 e^{(\rho_i-\tau_i)} \tag{28a}$$

$$\text{s.t.} \sum_{k\in\mathcal{K}_\mathcal{I}} \bar{\boldsymbol{u}}^H\mathbf{H}_i\boldsymbol{W}_k\mathbf{H}_i^H\bar{\boldsymbol{u}}+\sigma_z^2\bar{\boldsymbol{u}}^H\mathbf{T}_i\bar{\boldsymbol{u}}+\sigma_i^2\ge e^{\rho_i}, \quad \forall i\in\mathcal{K}_\mathcal{I}, \tag{28b}$$

$$\sum_{k\in\mathcal{K}_\mathcal{I}\setminus\{i\}} \bar{\boldsymbol{u}}^H\mathbf{H}_i\boldsymbol{W}_k\mathbf{H}_i^H\bar{\boldsymbol{u}}+\sigma_z^2\bar{\boldsymbol{u}}^H\mathbf{T}_i\bar{\boldsymbol{u}}+\sigma_i^2\le e^{\tau_i}, \quad \forall i\in\mathcal{K}_\mathcal{I}, \tag{28c}$$

$$\sum_{i\in\mathcal{K}_\mathcal{I}} \bar{\boldsymbol{u}}^H\mathbf{G}_j\boldsymbol{W}_i\mathbf{G}_j^H\bar{\boldsymbol{u}}+\sigma_z^2\bar{\boldsymbol{u}}^H\mathbf{Z}_j\bar{\boldsymbol{u}}\ge E_j, \quad \forall j\in\mathcal{K}_\mathcal{E}, \tag{28d}$$

$$\sum_{i\in\mathcal{K}_\mathcal{I}} \bar{\boldsymbol{u}}^H\mathbf{Q}_i\bar{\boldsymbol{u}}+\sigma_z^2\bar{\boldsymbol{u}}^H\mathbf{P}\bar{\boldsymbol{u}}\le P_\mathrm{I}, \tag{28e}$$

$$[\bar{\boldsymbol{u}}]_{N+1}=1. \tag{28f}$$

Note that the quadratic terms in (28b) and (28d), and the RHS of (28c) are all convex functions, thus making (28b)-(28d) non-convex. To deal with these constraints, we employ the SCA technique. Specifically, given the local feasible points $\bar{\boldsymbol{u}}^{(t)}$ and $\tau_i^{(t)}$ at the t-th iteration, by replacing the convex terms mentioned above with their respective first-order Taylor expansion-based lower bounds, we can obtain a convex subset of (28b)-(28d), as follows

$$\sum_{k\in\mathcal{K}_\mathcal{I}} \chi^{(t)}\left(\bar{\boldsymbol{u}},\mathbf{H}_i\boldsymbol{W}_k\mathbf{H}_i^H\right)+\sigma_z^2\chi^{(t)}(\bar{\boldsymbol{u}},\mathbf{T}_i)+\sigma_i^2\ge e^{\rho_i}, \quad \forall i\in\mathcal{K}_\mathcal{I}, \tag{29a}$$

$$\sum_{k\in\mathcal{K}_\mathcal{I}\setminus\{i\}} \bar{\boldsymbol{u}}^H\mathbf{H}_i\boldsymbol{W}_k\mathbf{H}_i^H\bar{\boldsymbol{u}}+\sigma_z^2\bar{\boldsymbol{u}}^H\mathbf{T}_i\bar{\boldsymbol{u}}+\sigma_i^2 \le e^{\tau_i^{(t)}}\left(\tau_i-\tau_i^{(t)}+1\right), \quad \forall i\in\mathcal{K}_\mathcal{I}, \tag{29b}$$

$$\sum_{i\in\mathcal{K}_\mathcal{I}} \chi^{(t)}\left(\bar{\boldsymbol{u}},\mathbf{G}_j\boldsymbol{W}_i\mathbf{G}_j^H\right)+\sigma_z^2\chi^{(t)}(\bar{\boldsymbol{u}},\mathbf{Z}_j)\ge E_j, \quad \forall j\in\mathcal{K}_\mathcal{E}, \tag{29c}$$

where $\chi^{(t)}(\bar{\boldsymbol{u}},\mathbf{B})\triangleq 2\mathrm{Re}\{\bar{\boldsymbol{u}}^H\mathbf{B}\bar{\boldsymbol{u}}^{(t)}\}-\left(\bar{\boldsymbol{u}}^{(t)}\right)^H\mathbf{B}\bar{\boldsymbol{u}}^{(t)}$, $\mathbf{B}\in\left\{\mathbf{H}_i\boldsymbol{W}_k\mathbf{H}_i^H,\mathbf{T}_i,\mathbf{G}_j\boldsymbol{W}_i\mathbf{G}_j^H,\mathbf{Z}_j\right\}$. As a result, a lower bound of the optimal solution to problem (28) can be obtained by solving the following convex QCQP with off-the-shelf convex optimization solvers, e.g., CVX [45].

$$\max_{\bar{\boldsymbol{u}},\{\rho_i,\tau_i\}} \sum_{i\in\mathcal{K}_\mathcal{I}} \mu_i \log_2 e^{(\rho_i-\tau_i)} \tag{30a}$$

$$\text{s.t.} \quad (29), (28\text{e}), (28\text{f}). \tag{30b}$$

C. Overall Algorithm

Based on Sections IV-A and IV-B, we propose an efficient algorithm for (P2-Eqv) by applying the AO method. Specifically, we solve (P2-Eqv-SDR2) by alternatingly solving problems (26) and (30) until convergence is achieved, where the obtained solution in each iteration is used as the input of the next iteration. The solution once convergence is reached is denoted by $\grave{\Pi}\triangleq\{\{\grave{\boldsymbol{W}}_i\},\grave{\boldsymbol{\Theta}},\{\grave{\rho}_i,\grave{\tau}_i\}\}$.

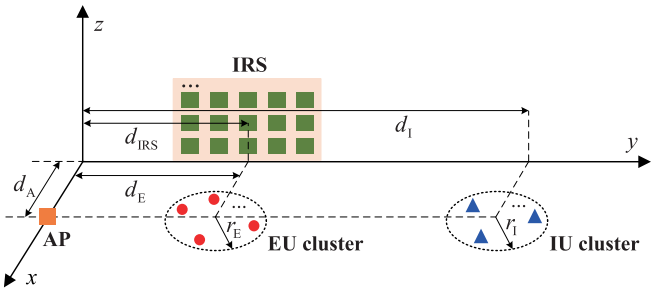

Fig. 2. Simulation setup.

If $\mathrm{rank}\big(\grave{\boldsymbol{W}}_i\big) \leq 1$ holds for all $i \in \mathcal{K}_{\mathcal{I}}$, the transmit precoder $\{\grave{\boldsymbol{w}}_i\}$ can be recovered from $\{\grave{\boldsymbol{W}}_i\}$ via the Cholesky decomposition. Otherwise, we define

$$\bar{\boldsymbol{w}}_i = \left(\boldsymbol{h}_i^H \grave{\boldsymbol{W}}_i \boldsymbol{h}_i\right)^{-1/2} \grave{\boldsymbol{W}}_i \boldsymbol{h}_i, \bar{\boldsymbol{W}}_i = \bar{\boldsymbol{w}}_i (\bar{\boldsymbol{w}}_i)^H, \quad \forall i \in \mathcal{K}_{\mathcal{I}} \backslash \{m\}, \tag{31a}$$

$$\bar{\boldsymbol{W}}_m = \sum_{i \in \mathcal{K}_{\mathcal{I}}} \grave{\boldsymbol{W}}_i - \sum_{i \in \mathcal{K}_{\mathcal{I}} \backslash \{m\}} \bar{\boldsymbol{W}}_i, \tag{31b}$$

where m can be any element in the set $\mathcal{K}_{\mathcal{I}}$. According to the proof of Theorem 2 in Appendix B, $\bar{\Pi} \triangleq \{\{\bar{\boldsymbol{W}}_i\}, \grave{\boldsymbol{\Theta}}, \{\grave{\rho}_i, \grave{\tau}_i\}\}$ is a feasible solution to (P2-Eqv-SDR2), and the objective values attained at $\grave{\Pi}$ and $\bar{\Pi}$ are the same. In this case, $\{\bar{\boldsymbol{w}}_i\}$ can be obtained by using (31) and performing the Gaussian randomization method over $\bar{\boldsymbol{W}}_m$.

Similar to the analyses in Sections III-A and III-C, the proposed algorithm is guaranteed to converge and the overall computational complexity is about [47], [48]

$$O\left[\mathcal{T}\left(\sqrt{b}\left(ab^3 + a^2b^2 + a^3\right)\log\left(\frac{1}{\varepsilon}\right) + \sqrt{c}\left(ca^2 + a^3\right)\ln\left(\frac{2cV}{\varepsilon}\right)\right)\right], \tag{32}$$

where $a \triangleq 2K_{\mathrm{I}} + K_{\mathrm{E}} + 2$, $b \triangleq M$, $c \triangleq 2K_{\mathrm{I}} + N + 1$, ε is the prescribed accuracy, V is a constant defined in [48], and $\mathcal{T}$ denotes the number of iterations needed for convergence.

V. Simulation Results

In this section, we demonstrate the effectiveness of the proposed algorithms with the aid of numerical simulations. As illustrated in Fig. 2, a three-dimensional (3D) coordinate setup is considered, where the AP and the IRS are located at $(d_{\mathrm{A}}, 0, 0)$ and $(0, d_{\mathrm{IRS}}, 0)$, respectively. The EUs and the IUs are randomly and uniformly distributed within two disks centered at $(d_{\mathrm{A}}, d_{\mathrm{E}}, 0)$ and $(d_{\mathrm{A}}, d_{\mathrm{I}}, 0)$ with radii equal to r_{E} and r_{I}, respectively. The system is assumed to operate on a carrier frequency of 750 MHz, with a wavelength $\lambda_c = 0.4$ meter (m) [24], [35]. The large-scale path loss is modeled as $L(d) = C_0 \left(d/D_0\right)^{(-\alpha)}$ [5], where $C_0 = \left(\frac{\lambda_c}{4\pi}\right)^2$ is the path loss at the reference distance $D_0 = 1$ m, d denotes the link distance, and α represents the path loss exponent. The path loss exponents of the AP-IRS, IRS-user, and AP-user links are set equal to $\alpha_{\mathrm{AI}} = 2.2$ [23], $\alpha_{\mathrm{Iu}} = 2.2$ [23], and $\alpha_{\mathrm{Au}} = 3.2$, respectively. We assume that the AP-IRS and the IRS-user links experience Rician fading with a Rician factor of 3 dB, while the AP-user links undergo Rayleigh fading [22]. In addition, we set $\alpha_j = 1$, $\forall j \in \mathcal{K}_{\mathcal{E}}$ in (P1) and $\mu_i = 1$, $\forall i \in \mathcal{K}_{\mathcal{I}}$ in (P2), i.e., the sum-power harvested by all the EUs and the sum-rate of all the IUs are considered, respectively [23], [25]. Unless otherwise specified, other system parameters are set as follows: $\sigma_z^2 = \sigma_i^2 = -80$ dBm [30], $\gamma_i = \gamma$, $\forall i \in \mathcal{K}_{\mathcal{I}}$, $E_j = E$, $\forall j \in \mathcal{K}_{\mathcal{E}}$, $N = 50$, $M = 5$, $d_{\mathrm{A}} = 3$ m, $d_{\mathrm{I}} = 100$ m, and $r_{\mathrm{E}} = r_{\mathrm{I}} = 2$ m.

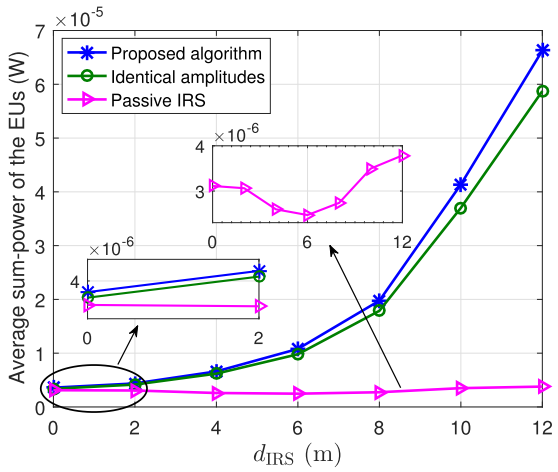

Fig. 3. Average sum-power of the EUs versus the y-axis coordinate value of the IRS.

For comparison purposes, we focus on the following two benchmark schemes: 1) Identical amplitudes: all active elements are assumed to have identical amplitudes, i.e., $\beta_n = \beta$, $\forall n \in \mathcal{N}$, and β is optimized; 2) Passive IRS: we set $\beta_n = 1$, $\forall n \in \mathcal{N}$, neglect the noise introduced by the IRS, and remove the amplification power constraint. Moreover, for a fair comparison, we assume that the AP's total transmit power budget is $P_{\mathrm{A}} + P_{\mathrm{I}}$ in this benchmark scheme. The simulation results are obtained by averaging 100 independent realizations of the channels and the users' locations.

A. Weighted Sum-Power Maximization

1) Special Case With No IUs: We first investigate a special case of the weighted sum-power maximization problem (P1) where there exist no IUs, i.e., $\mathcal{K}_{\mathcal{I}} = \emptyset$. By varying the value of d_{IRS}, we examine in Fig. 3 the average sum-power of $K_{\mathrm{E}} = 4$ EUs with $P_{\mathrm{A}} = 23$ dBm, $P_{\mathrm{I}} = 5$ dBm, and $d_{\mathrm{E}} = 12$ m. When deploying a passive IRS, as expected, it is observed that the EUs harvest the lowest sum-power when the IRS is located far from both the AP and the EU cluster (i.e., $d_{\mathrm{IRS}} = 6$ m) due to the product path loss attenuation law. When deploying an active IRS, in contrast, the sum-power of EUs increases drastically as the IRS moves closer to the EU cluster, since the incident signal power at the IRS becomes weaker with increasing d_{IRS}, the active IRS can provide higher amplification gain according to constraint (8c), which compensates for the product path loss attenuation and contributes to an increase in the sum-power harvested by the EUs. This result indicates that to reap the full benefits of an active IRS, we should deploy it close to the EUs. Besides,

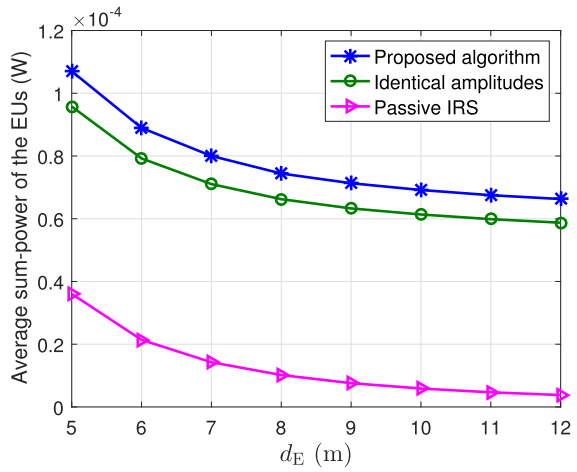

Fig. 4. Average sum-power of the EUs versus the distance between the AP and the center of the disk of the EU cluster, where $d_{\mathrm{IRS}} = d_{\mathrm{E}}$.

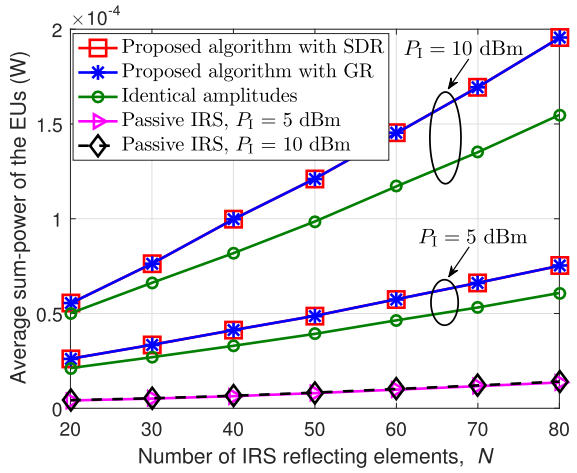

Fig. 5. Average sum-power of the EUs versus the number of IRS elements.

it can been seen that the proposed algorithm outperforms the scheme with identical amplitudes at the active IRS as well as the scheme employing a passive IRS. The performance loss caused by adopting identical amplitudes for all elements shows the importance of properly designing the amplitudes at the active IRS for enhancing the system performance.

To further demonstrate the benefits brought by the active IRS to WPT, we plot in Fig. 4 the average sum-power of the EUs versus the distance between the AP and the center of the disk of the EU cluster, where the IRS moves with the EU cluster to maintain the condition $d_{\mathrm{IRS}} = d_{\mathrm{E}}$. The other parameters are the same as those in Fig. 3. As can be seen, by deploying an active IRS around the EUs, their sum harvested power is observably improved compared to the case with a passive IRS. This observation suggests that deploying an active IRS is more effective than deploying a passive IRS in extending the WPT operating range.

2) General Case With EUs and IUs Coexisting: Next, we consider the general case of (P1) where both the EUs and the IUs exist. In Fig. 5, we show the average sum-power of the EUs versus the number of IRS elements with $K_{\mathrm{E}} = 4$,

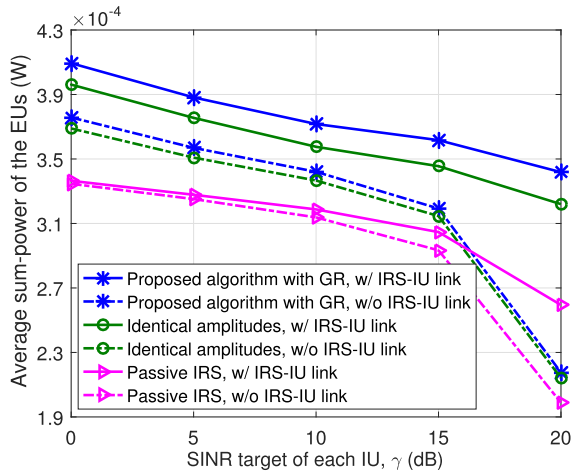

Fig. 6. Average sum-power of the EUs versus the SINR target of each IU.

$K_{\mathrm{I}} = 2$, $P_{\mathrm{A}} = 23$ dBm, $\gamma = 5$ dB, and $d_{\mathrm{IRS}} = d_{\mathrm{E}} = 8$ m. Note that the "Proposed algorithm with SDR" corresponds to the solution when the proposed algorithm for the SDR problem in (17) converges, while the "Proposed algorithm with GR" utilizes the Gaussian randomization method to construct a rank-one $\boldsymbol{U}$ based on the solution obtained with the SDR method. It is observed that the performance of the proposed algorithm with GR closely approaches that achieved by the SDR method. One can also conclude from Fig. 5 that the deployment of an active IRS is more suitable for application to space-limited scenarios, since it can significantly reduce the required surface size for achieving a given performance level. Furthermore, we observe that increasing N widens the performance gap between the proposed algorithm and the other two benchmark schemes, as the former offers a better utilization of the system resources. Finally, we can see that a larger P_{I} leads to a better performance of the SWIPT system with an active IRS. This is excepted since an active IRS can provide a higher amplification gain for a larger value of P_{I}. In contrast, the increase of P_{I} only brings a negligible performance gain to the passive IRS scheme as the value of P_{A}, which is significantly larger than the two different values of P_{I}, dominates the performance of this scheme.

In Fig. 6, we study the average sum-power of the EUs versus the SINR target of each IU with $P_{\mathrm{A}} = 30$ dBm and $P_{\mathrm{I}} = 10$ dBm (other parameters are set to be the same as in Fig. 5). Two cases with and without the IRS-IU link are considered. As expected, the proposed algorithm significantly outperforms the other two benchmark schemes over the whole considered SINR regime. Another observation is that the performance gap between the two cases of the proposed algorithm is much larger than that of the passive IRS scheme, which shows the advantage of deploying an active IRS for effective WIT even when the IUs are far away from the IRS.

B. Weighted Sum-Rate Maximization

In this subsection, we evaluate the performance of the proposed algorithm for the weighted sum-rate maximization problem (P2). Fig. 7 illustrates the average sum-rate of IUs

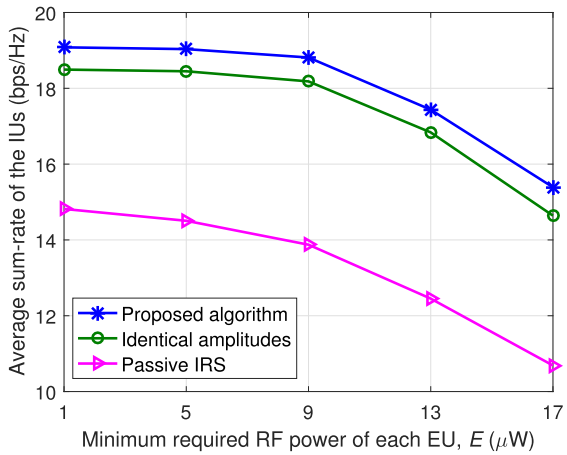

Fig. 7. Average sum-rate of the IUs versus the minimum required RF power of each EU.

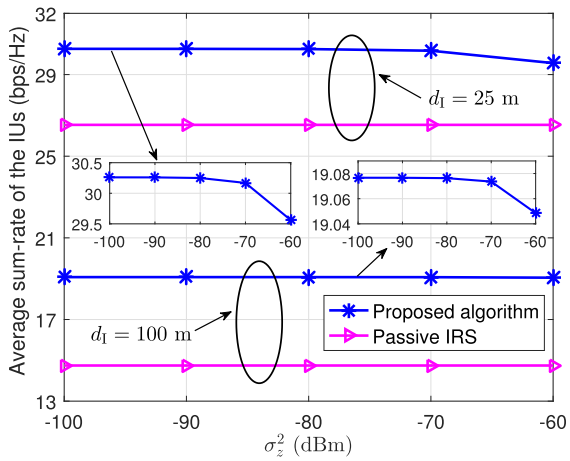

Fig. 9. Average sum-rate of the IUs versus the noise variance of the active IRS.

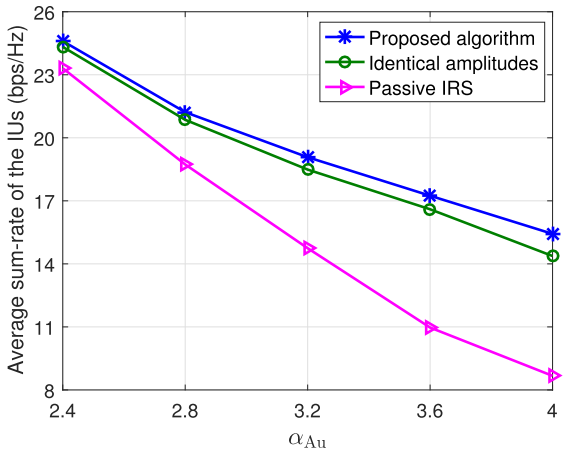

Fig. 8. Average sum-rate of the IUs versus the path loss exponent of the AP-user link.

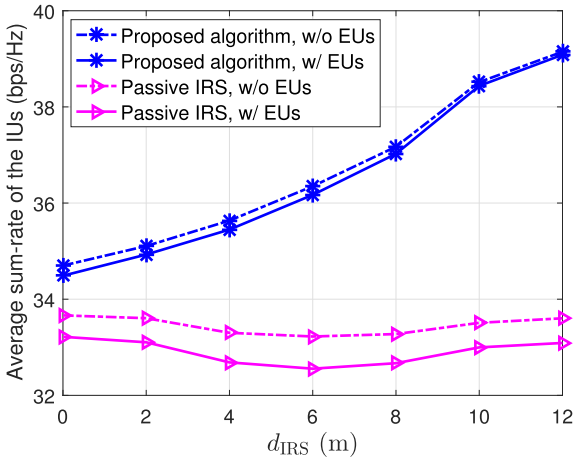

Fig. 10. Average sum-rate of the IUs versus the y-axis coordinate value of the IRS.

versus the minimum required RF power of each EU with $K_{\rm E} = K_{\rm I} = 2$, $P_{\rm A} = 30$ dBm, $P_{\rm I} = 10$ dBm, and $d_{\rm IRS} = d_{\rm E} = 8$ m. It is observed that the proposed algorithm performs much better than the passive IRS scheme, and the performance gap is larger with the increase of E. This again indicates that the deployment of an active IRS is beneficial to both WIT and WPT.

Under the same setup as in Fig. 7, we study in Fig. 8 the impact of the path loss exponent of the AP-user direct link on the performance of different schemes when $E = 3$ μW. It can be seen that deploying an active IRS is more advantageous than deploying a passive IRS regardless of the value of $\alpha_{\rm Au}$. In addition, the performance gap between the proposed algorithm and the passive IRS scheme increases markedly with $\alpha_{\rm Au}$. This is expected since the performance of both schemes is dominated by the AP-user direct link when $\alpha_{\rm Au}$ is small while by the AP-IRS-user reflected link when $\alpha_{\rm Au}$ is large.

In Fig. 9, the impact of the noise variance of the active IRS on the performance of the proposed algorithm is investigated. Here, we set $E = 3$ μW and the other parameters are the same as those in Fig. 7. We can observe that even if σ_z^2 is very large, an active IRS can outperform a passive IRS via a proper joint optimization of the transmit and reflect beamforming. Moreover, the performance degradation of the proposed algorithm due to the increase of σ_z^2 is very small, sometimes even negligible when the IUs are far away from the IRS (i.e., $d_{\rm I} = 100$ m).

Finally, to gain more insights, we consider a setup where $d_{\rm I} = d_{\rm E} = 12$ m, i.e., the EUs and the IUs are randomly and uniformly located in the same disk centered at $(3, 12, 0)$ with radius 2 m. In Fig. 10, we compare the average sum-rate achieved by the proposed algorithm and the passive IRS scheme for both cases with and without the EUs versus the y-axis coordinate value of the IRS when $E = 1$ μW. The other simulation parameters are the same as those in Fig. 7. In addition to observations similar to those in Fig. 3, we can see that the existence of the EUs brings a much smaller performance degradation to the proposed algorithm than to the scheme employing a passive IRS, especially when the active IRS is deployed in the proximity of the users. This result further shows the superiority of deploying an active IRS in enhancing the performance of SWIPT systems with both EUs and IUs coexisting.

VI. Conclusion

In this paper, we studied the weighted sum-power and sum-rate maximization problems in an active IRS-assisted SWIPT system. Specifically, the first problem aimed to maximize the weighted sum-power harvested by the EUs while meeting the specified SINR targets at the IUs, and the second problem was intended to maximize the weighted sum-rate of the IUs while satisfying the EH requirements at the EUs. In both problems, the transmit precoder at the AP and the reflection-coefficient matrix at the IRS were jointly optimized. Interestingly, it was rigorously proved that there is no loss of optimality in removing dedicated energy beams in the SDR reformulations of both optimization problems. Based on these results, efficient suboptimal algorithms were proposed for the resulting problems. Numerical results verified that, compared with the benchmark scheme using a passive IRS, the proposed designs with an active IRS are able to significantly enhance the performance of both the EUs and the IUs. Useful insights on the appropriate deployment of an active IRS were also identified, providing helpful guidance for the practical design and implementation.

Appendix A
Proof of Theorem 1

To prove Theorem 1, we aim to show that (P1-SDR1) shares the same optimal value with the following problem (P1-SDR2) and that an optimal solution satisfying $\mathrm{rank}\,(\boldsymbol{W}_i^*)=1$, $\forall i\in\mathcal{K}_{\mathcal{I}}$ exists for (P1-SDR2):

$$\begin{aligned}
\text{(P1-SDR2)}:\ &\max_{\{\boldsymbol{W}_{i\in\mathbb{H}^M}\},\,\boldsymbol{\Theta}}\ \sum_{i\in\mathcal{K}_{\mathcal{I}}}\mathrm{tr}\left(\boldsymbol{S}\boldsymbol{W}_i\right)\\
&\qquad+\sum_{j\in\mathcal{K}_{\mathcal{E}}}\alpha_j\sigma_z^2\left\|\boldsymbol{g}_{r,j}^H\boldsymbol{\Theta}\right\|^2 &\text{(33a)}\\
&\text{s.t.}\ \frac{\mathrm{tr}\left(\boldsymbol{h}_i\boldsymbol{h}_i^H\boldsymbol{W}_i\right)}{\gamma_i}-\sum_{k\in\mathcal{K}_{\mathcal{I}}\backslash\{i\}}\mathrm{tr}\left(\boldsymbol{h}_i\boldsymbol{h}_i^H\boldsymbol{W}_k\right)-\bar{\sigma}_i^2\geq 0,\\
&\qquad\qquad\forall i\in\mathcal{K}_{\mathcal{I}}, &\text{(33b)}\\
&\sum_{i\in\mathcal{K}_{\mathcal{I}}}\mathrm{tr}\left(\boldsymbol{W}_i\right)\leq P_{\mathrm{A}},\ \sum_{i\in\mathcal{K}_{\mathcal{I}}}\mathrm{tr}\left(\boldsymbol{C}\boldsymbol{W}_i\right)\leq\bar{P}_{\mathrm{I}}, &\text{(33c)}\\
&\boldsymbol{W}_i\succeq\boldsymbol{0},\quad\forall i\in\mathcal{K}_{\mathcal{I}}. &\text{(33d)}
\end{aligned}$$

Denote ζ_1^* and ζ_2^* as the optimal objective values of (P1-SDR1) and (P1-SDR2), respectively. Suppose that $\{\{\hat{\boldsymbol{W}}_i\},\hat{\boldsymbol{W}}_{\mathrm{E}},\hat{\boldsymbol{\Theta}}\}$ is an arbitrary optimal solution to (P1-SDR1) corresponding to ζ_1^*. Obviously, $\zeta_1^*\geq\zeta_2^*$ since (P1-SDR2) is a special case of (P1-SDR1) with $\boldsymbol{W}_{\mathrm{E}}=\boldsymbol{0}$. Next, we prove that $\zeta_1^*\leq\zeta_2^*$ also holds, building on the insight that by adding $\hat{\boldsymbol{W}}_{\mathrm{E}}$ into any $\hat{\boldsymbol{W}}_i$, we can construct a feasible solution to (P1-SDR2) that achieves the same objective value as ζ_1^*. Specifically, let $\tilde{\boldsymbol{W}}_m=\hat{\boldsymbol{W}}_m+\hat{\boldsymbol{W}}_{\mathrm{E}}$ for any $m\in\mathcal{K}_{\mathcal{I}}$ and $\tilde{\boldsymbol{W}}_i=\hat{\boldsymbol{W}}_i$, $\forall i\in\mathcal{K}_{\mathcal{I}}\backslash\{m\}$. It is easy to verify that the constraints in (33c) and (33d) hold for the new solution set $\tilde{\Gamma}\triangleq\{\{\tilde{\boldsymbol{W}}_i\},\hat{\boldsymbol{\Theta}}\}$ and the objective value of (P1-SDR2) achieved by $\tilde{\Gamma}$ equals ζ_1^*. Then, we show that $\tilde{\Gamma}$ also fulfills the constraints in (33b). To this end, the following two cases are considered:

1) For $m\in\mathcal{K}_{\mathcal{I}}$: We have

$$\begin{aligned}
&\frac{\mathrm{tr}\left(\boldsymbol{h}_m\boldsymbol{h}_m^H\tilde{\boldsymbol{W}}_m\right)}{\gamma_m}-\sum_{k\in\mathcal{K}_{\mathcal{I}}\backslash\{m\}}\mathrm{tr}\left(\boldsymbol{h}_m\boldsymbol{h}_m^H\tilde{\boldsymbol{W}}_k\right)-\bar{\sigma}_m^2\\
&=\frac{\mathrm{tr}\left(\boldsymbol{h}_m\boldsymbol{h}_m^H\hat{\boldsymbol{W}}_m\right)}{\gamma_m}+\frac{\mathrm{tr}\left(\boldsymbol{h}_m\boldsymbol{h}_m^H\hat{\boldsymbol{W}}_E\right)}{\gamma_m}\\
&\quad-\sum_{k\in\mathcal{K}_{\mathcal{I}}\backslash\{m\}}\mathrm{tr}\left(\boldsymbol{h}_m\boldsymbol{h}_m^H\hat{\boldsymbol{W}}_k\right)-\bar{\sigma}_m^2\\
&\overset{(a)}{\geq}\frac{\mathrm{tr}\left(\boldsymbol{h}_m\boldsymbol{h}_m^H\hat{\boldsymbol{W}}_m\right)}{\gamma_m}-\mathrm{tr}\left(\boldsymbol{h}_m\boldsymbol{h}_m^H\hat{\boldsymbol{W}}_E\right)\\
&\quad-\sum_{k\in\mathcal{K}_{\mathcal{I}}\backslash\{m\}}\mathrm{tr}\left(\boldsymbol{h}_m\boldsymbol{h}_m^H\hat{\boldsymbol{W}}_k\right)-\bar{\sigma}_m^2\overset{(b)}{\geq}0,
\end{aligned}\tag{34}$$

where (a) uses $\hat{\boldsymbol{W}}_E\succeq\boldsymbol{0}$ and (b) holds due to (14b).

2) For Any $i\in\mathcal{K}_{\mathcal{I}}\backslash\{m\}$: It follows that

$$\begin{aligned}
&\frac{\mathrm{tr}\left(\boldsymbol{h}_i\boldsymbol{h}_i^H\tilde{\boldsymbol{W}}_i\right)}{\gamma_i}-\sum_{k\in\mathcal{K}_{\mathcal{I}}\backslash\{i\}}\mathrm{tr}\left(\boldsymbol{h}_i\boldsymbol{h}_i^H\tilde{\boldsymbol{W}}_k\right)-\bar{\sigma}_i^2\\
&=\frac{\mathrm{tr}\left(\boldsymbol{h}_i\boldsymbol{h}_i^H\tilde{\boldsymbol{W}}_i\right)}{\gamma_i}-\sum_{k\in\mathcal{K}_{\mathcal{I}}\backslash\{i,m\}}\mathrm{tr}\left(\boldsymbol{h}_i\boldsymbol{h}_i^H\tilde{\boldsymbol{W}}_k\right)\\
&\quad-\mathrm{tr}\left(\boldsymbol{h}_i\boldsymbol{h}_i^H\tilde{\boldsymbol{W}}_m\right)-\bar{\sigma}_i^2\\
&=\frac{\mathrm{tr}\left(\boldsymbol{h}_i\boldsymbol{h}_i^H\hat{\boldsymbol{W}}_i\right)}{\gamma_i}-\sum_{k\in\mathcal{K}_{\mathcal{I}}\backslash\{i\}}\mathrm{tr}\left(\boldsymbol{h}_i\boldsymbol{h}_i^H\hat{\boldsymbol{W}}_k\right)\\
&\quad-\mathrm{tr}\left(\boldsymbol{h}_i\boldsymbol{h}_i^H\hat{\boldsymbol{W}}_E\right)-\bar{\sigma}_i^2\geq 0,
\end{aligned}\tag{35}$$

where the inequality follows from (14b).

Based on the above, we have

$$\frac{\mathrm{tr}\left(\boldsymbol{h}_i\boldsymbol{h}_i^H\tilde{\boldsymbol{W}}_i\right)}{\gamma_i}-\sum_{k\in\mathcal{K}_{\mathcal{I}}\backslash\{i\}}\mathrm{tr}\left(\boldsymbol{h}_i\boldsymbol{h}_i^H\tilde{\boldsymbol{W}}_k\right)-\bar{\sigma}_i^2\geq 0,\quad\forall i\in\mathcal{K}_{\mathcal{I}},\tag{36}$$

which indicates that constraint (33b) also holds for $\tilde{\Gamma}$. As a result, $\tilde{\Gamma}$ is a feasible solution to (P1-SDR2). For (P1-SDR2), since its objective value achieved by the feasible solution $\tilde{\Gamma}$ is equal to ζ_1^* and must not be greater than its optimal objective value ζ_2^*, we have $\zeta_1^*\leq\zeta_2^*$. Since $\zeta_1^*\geq\zeta_2^*$, we have $\zeta_1^*=\zeta_2^*$.

Furthermore, according to [46, Theorem 3.2], there always exists an optimal solution to (P1-SDR2) satisfying $\sum_{i\in\mathcal{K}_{\mathcal{I}}}\left(\mathrm{rank}\,(\boldsymbol{W}_i^*)\right)^2\leq K_{\mathrm{I}}+2$ under any $\boldsymbol{\Theta}$. Meanwhile, for $\gamma_i>0$, $\forall i\in\mathcal{K}_{\mathcal{I}}$, there must be $\boldsymbol{W}_i^*\neq\boldsymbol{0}$ or equivalently $\mathrm{rank}\,(\boldsymbol{W}_i^*)\geq 1$. Then, it follows that $\mathrm{rank}\,(\boldsymbol{W}_i^*)=1$, $\forall i\in\mathcal{K}_{\mathcal{I}}$ should exist for (P1-SDR2). Combing the above results completes the proof.

APPENDIX B
PROOF OF THEOREM 2

We prove Theorem 2 by showing that (P2-Eqv-SDR1) shares the same optimal value with the following problem (P2-Eqv-SDR2) and that there always exists an optimal solution to (P2-Eqv-SDR2) satisfying $\mathrm{rank}\,(\boldsymbol{W}_i^*) \le 1, \forall i \in \mathcal{K}_{\mathcal{I}}'$, where $\mathcal{K}_{\mathcal{I}}' \subseteq \mathcal{K}_{\mathcal{I}}$ and $|\mathcal{K}_{\mathcal{I}}'| \ge K_{\mathrm{I}} - 1$:

(P2-Eqv-SDR2) :

$$\max_{\substack{\{\boldsymbol{W}_i \in \mathbb{H}^M\},\\ \boldsymbol{\Theta},\{\rho_i,\tau_i\}}} \sum_{i\in\mathcal{K}_{\mathcal{I}}} \mu_i \log_2 e^{(\rho_i-\tau_i)} \tag{37a}$$

$$\text{s.t.} \sum_{k\in\mathcal{K}_{\mathcal{I}}} \mathrm{tr}\left(\boldsymbol{h}_i\boldsymbol{h}_i^H\boldsymbol{W}_k\right) + \bar{\sigma}_i^2 \ge e^{\rho_i}, \quad \forall i \in \mathcal{K}_{\mathcal{I}}, \tag{37b}$$

$$\sum_{k\in\mathcal{K}_{\mathcal{I}}\backslash\{i\}} \mathrm{tr}\left(\boldsymbol{h}_i\boldsymbol{h}_i^H\boldsymbol{W}_k\right) + \bar{\sigma}_i^2 \le e^{\tau_i}, \quad \forall i \in \mathcal{K}_{\mathcal{I}}, \tag{37c}$$

$$\sum_{i\in\mathcal{K}_{\mathcal{I}}} \mathrm{tr}\left(\boldsymbol{g}_j\boldsymbol{g}_j^H\boldsymbol{W}_i\right) \ge \bar{E}_j, \quad \forall j \in \mathcal{K}_{\mathcal{E}}, \tag{37d}$$

$$\sum_{i\in\mathcal{K}_{\mathcal{I}}} \mathrm{tr}\left(\boldsymbol{W}_i\right) \le P_{\mathrm{A}}, \ \sum_{i\in\mathcal{K}_{\mathcal{I}}} \mathrm{tr}\left(\boldsymbol{C}\boldsymbol{W}_i\right) \le \bar{P}_{\mathrm{I}}, \tag{37e}$$

$$\boldsymbol{W}_i \succeq \boldsymbol{0}, \quad \forall i \in \mathcal{K}_{\mathcal{I}}. \tag{37f}$$

Particularly, the proof of the equivalence between (P2-Eqv-SDR1) and (P2-Eqv-SDR2) is similar to that of the equivalence between (P1-SDR1) and (P1-SDR2) given in Appendix A. Therefore, the details are omitted due to the space limitation.

The remaining part is to prove that (P2-Eqv-SDR2) has an optimal solution where at least $K_{\mathrm{I}} - 1$ beamforming matrices $\{\boldsymbol{W}_i^*\}$ satisfy $\mathrm{rank}\,(\boldsymbol{W}_i^*) \le 1$. Let $\check{\Xi} \triangleq \{\{\check{\boldsymbol{W}}_i\}, \check{\boldsymbol{\Theta}}, \{\check{\rho}_i, \check{\tau}_i\}\}$ be an arbitrary optimal solution to (P2-Eqv-SDR2), where $\mathrm{rank}\left(\check{\boldsymbol{W}}_i\right) > 1$ holds for more than one $i \in \mathcal{K}_{\mathcal{I}}$. Then, we construct $\Xi^* \triangleq \{\{\boldsymbol{W}_i^*\}, \boldsymbol{\Theta}^*, \{\rho_i^*, \tau_i^*\}\}$ from $\check{\Xi}$ with[7]

$$\boldsymbol{\Theta}^* = \check{\boldsymbol{\Theta}}, \rho_i^* = \check{\rho}_i, \tau_i^* = \check{\tau}_i, \quad \forall i \in \mathcal{K}_{\mathcal{I}}, \tag{38}$$

$$\boldsymbol{w}_i^* = \left(\boldsymbol{h}_i^H\check{\boldsymbol{W}}_i\boldsymbol{h}_i\right)^{-1/2}\check{\boldsymbol{W}}_i\boldsymbol{h}_i, \boldsymbol{W}_i^* = \boldsymbol{w}_i^*(\boldsymbol{w}_i^*)^H, \quad \forall i \in \mathcal{K}_{\mathcal{I}}\backslash\{m\}, \tag{39}$$

$$\boldsymbol{W}_m^* = \sum_{i\in\mathcal{K}_{\mathcal{I}}} \check{\boldsymbol{W}}_i - \sum_{i\in\mathcal{K}_{\mathcal{I}}\backslash\{m\}} \boldsymbol{W}_i^*, \tag{40}$$

where m can be any element in the set $\mathcal{K}_{\mathcal{I}}$. It is clear that $\mathrm{rank}\,(\boldsymbol{W}_i^*) \le 1$ and $\boldsymbol{W}_i^* \succeq \boldsymbol{0}$, $\forall i \in \mathcal{K}_{\mathcal{I}}\backslash\{m\}$. In the following, we show that Ξ^* is also an optimal solution to (P2-Eqv-SDR2).

First, for any $\boldsymbol{D} \in \mathbb{C}^{M\times M}$, it holds that

$$\sum_{i\in\mathcal{K}_{\mathcal{I}}} \mathrm{tr}\left(\boldsymbol{D}\boldsymbol{W}_i^*\right) = \sum_{i\in\mathcal{K}_{\mathcal{I}}\backslash\{m\}} \mathrm{tr}\left(\boldsymbol{D}\boldsymbol{W}_i^*\right) + \mathrm{tr}\left(\boldsymbol{D}\boldsymbol{W}_m^*\right) = \sum_{i\in\mathcal{K}_{\mathcal{I}}} \mathrm{tr}\left(\boldsymbol{D}\check{\boldsymbol{W}}_i\right). \tag{41}$$

Then, it is easy to see that constraints (37b), (37d), and (37e) hold for Ξ^*.

Next, for any $\boldsymbol{q} \in \mathbb{C}^{M\times 1}$, we have

$$\begin{aligned}
&\boldsymbol{q}^H\left(\check{\boldsymbol{W}}_i - \boldsymbol{W}_i^*\right)\boldsymbol{q} \\
&= \boldsymbol{q}^H\check{\boldsymbol{W}}_i\boldsymbol{q} - \left(\boldsymbol{h}_i^H\check{\boldsymbol{W}}_i\boldsymbol{h}_i\right)^{-1}\left|\boldsymbol{q}^H\check{\boldsymbol{W}}_i\boldsymbol{h}_i\right|^2 \\
&\ge \boldsymbol{q}^H\check{\boldsymbol{W}}_i\boldsymbol{q} - \left(\boldsymbol{h}_i^H\check{\boldsymbol{W}}_i\boldsymbol{h}_i\right)^{-1}\left(\boldsymbol{h}_i^H\check{\boldsymbol{W}}_i\boldsymbol{h}_i\right)\left(\boldsymbol{q}^H\check{\boldsymbol{W}}_i\boldsymbol{q}\right) \\
&= 0, \quad \forall i \in \mathcal{K}_{\mathcal{I}}\backslash\{m\},
\end{aligned} \tag{42}$$

where the inequality holds due to the Cauchy-Schwarz inequality. It then follows that $\check{\boldsymbol{W}}_i - \boldsymbol{W}_i^* \succeq \boldsymbol{0}$, $\forall i \in \mathcal{K}_{\mathcal{I}}\backslash\{m\}$. Subsequently, we have

$$\begin{aligned}
\boldsymbol{W}_m^* &= \sum_{i\in\mathcal{K}_{\mathcal{I}}} \check{\boldsymbol{W}}_i - \sum_{i\in\mathcal{K}_{\mathcal{I}}\backslash\{m\}} \boldsymbol{W}_i^* \\
&= \check{\boldsymbol{W}}_m + \sum_{i\in\mathcal{K}_{\mathcal{I}}\backslash\{m\}} \left(\check{\boldsymbol{W}}_i - \boldsymbol{W}_i^*\right) \succeq \boldsymbol{0}.
\end{aligned} \tag{43}$$

Therefore, constraint (37f) holds for Ξ^*.

It remains to prove that Ξ^* ensures constraint (37c). To show this, we consider the following two cases:

1) For $m \in \mathcal{K}_{\mathcal{I}}$: In this case, it follows that

$$\begin{aligned}
&\sum_{k\in\mathcal{K}_{\mathcal{I}}\backslash\{m\}} \mathrm{tr}\left(\boldsymbol{h}_m\boldsymbol{h}_m^H\check{\boldsymbol{W}}_k\right) - \sum_{k\in\mathcal{K}_{\mathcal{I}}\backslash\{m\}} \mathrm{tr}\left(\boldsymbol{h}_m\boldsymbol{h}_m^H\boldsymbol{W}_k^*\right) \\
&= \sum_{k\in\mathcal{K}_{\mathcal{I}}\backslash\{m\}} \boldsymbol{h}_m^H\left(\check{\boldsymbol{W}}_k - \boldsymbol{W}_k^*\right)\boldsymbol{h}_m \ge 0,
\end{aligned} \tag{44}$$

where the inequality follows from (42).

2) For Any $i \in \mathcal{K}_{\mathcal{I}}\backslash\{m\}$: First of all, it holds that $\boldsymbol{h}_i^H\boldsymbol{W}_i^*\boldsymbol{h}_i = \boldsymbol{h}_i^H\boldsymbol{w}_i^*(\boldsymbol{w}_i^*)^H\boldsymbol{h}_i = \boldsymbol{h}_i^H\check{\boldsymbol{W}}_k\boldsymbol{h}_i$, $\forall i \in \mathcal{K}_{\mathcal{I}}\backslash\{m\}$. This, together with (40), yields

$$\begin{aligned}
&\sum_{k\in\mathcal{K}_{\mathcal{I}}\backslash\{i\}} \mathrm{tr}\left(\boldsymbol{h}_i\boldsymbol{h}_i^H\check{\boldsymbol{W}}_k\right) - \sum_{k\in\mathcal{K}_{\mathcal{I}}\backslash\{i\}} \mathrm{tr}\left(\boldsymbol{h}_i\boldsymbol{h}_i^H\boldsymbol{W}_k^*\right) \\
&= \sum_{k\in\mathcal{K}_{\mathcal{I}}\backslash\{i\}} \mathrm{tr}\left(\boldsymbol{h}_i\boldsymbol{h}_i^H\check{\boldsymbol{W}}_k\right) - \left(\sum_{k\in\mathcal{K}_{\mathcal{I}}\backslash\{i,m\}} \mathrm{tr}\left(\boldsymbol{h}_i\boldsymbol{h}_i^H\boldsymbol{W}_k^*\right)\right. \\
&\quad \left. + \sum_{k\in\mathcal{K}_{\mathcal{I}}} \mathrm{tr}\left(\boldsymbol{h}_i\boldsymbol{h}_i^H\check{\boldsymbol{W}}_k\right) - \sum_{k\in\mathcal{K}_{\mathcal{I}}\backslash\{m\}} \mathrm{tr}\left(\boldsymbol{h}_i\boldsymbol{h}_i^H\boldsymbol{W}_k^*\right)\right) \\
&= \sum_{k\in\mathcal{K}_{\mathcal{I}}\backslash\{i\}} \mathrm{tr}\left(\boldsymbol{h}_i\boldsymbol{h}_i^H\check{\boldsymbol{W}}_k\right) - \sum_{k\in\mathcal{K}_{\mathcal{I}}} \mathrm{tr}\left(\boldsymbol{h}_i\boldsymbol{h}_i^H\check{\boldsymbol{W}}_k\right) \\
&\quad + \mathrm{tr}\left(\boldsymbol{h}_i\boldsymbol{h}_i^H\boldsymbol{W}_i^*\right) \\
&= -\mathrm{tr}\left(\boldsymbol{h}_i\boldsymbol{h}_i^H\check{\boldsymbol{W}}_i\right) + \mathrm{tr}\left(\boldsymbol{h}_i\boldsymbol{h}_i^H\boldsymbol{W}_i^*\right) = 0.
\end{aligned} \tag{45}$$

With (44) and (45), we have

$$\sum_{k\in\mathcal{K}_{\mathcal{I}}\backslash\{i\}} \mathrm{tr}\left(\boldsymbol{h}_i\boldsymbol{h}_i^H\boldsymbol{W}_k^*\right) + \bar{\sigma}_i^2$$

[7]For any $\check{\boldsymbol{W}}_i = \boldsymbol{0}$, $i \in \mathcal{K}_{\mathcal{I}}\backslash\{m\}$, let $\boldsymbol{W}_i^* = \boldsymbol{0}$.

$$\leq \sum_{k\in\mathcal{K}_{\mathcal{I}}\backslash\{i\}} \mathrm{tr}\left(\boldsymbol{h}_i\boldsymbol{h}_i^H\check{\boldsymbol{W}}_k\right)+\bar{\sigma}_i^2 \leq e^{\check{y}_i}$$
$$= e^{y_i^*}, \quad \forall i\in\mathcal{K}_{\mathcal{I}}, \tag{46}$$

namely constraint (37c) holds for Ξ^*.

Finally, we note that the objective values in (37a) achieved by Ξ^* and $\check{\Xi}$ are identical.

With the derivation above, it is verified that Ξ^* is an optimal solution to (P2-Eqv-SDR2), where $\mathrm{rank}\,(\boldsymbol{W}_i^*)\leq 1$ holds for no less than $(K_{\mathrm{I}}-1)$ $i\in\mathcal{K}_{\mathcal{I}}$. Theorem 2 is thus proved.

REFERENCES

[1] Q. Wu, X. Guan, and R. Zhang, "Intelligent reflecting surface-aided wireless energy and information transmission: An overview," *Proc. IEEE*, vol. 110, no. 1, pp. 150–170, Jan. 2022.

[2] J. Xu, L. Liu, and R. Zhang, "Multiuser MISO beamforming for simultaneous wireless information and power transfer," 2013, *arXiv:1303.1911*.

[3] S. Zhang, Q. Wu, S. Xu, and G. Y. Li, "Fundamental green tradeoffs: Progresses, challenges, and impacts on 5G networks," *IEEE Commun. Surveys Tuts.*, vol. 19, no. 1, pp. 33–56, 1st Quat., 2017.

[4] Q. Wu and R. Zhang, "Towards smart and reconfigurable environment: Intelligent reflecting surface aided wireless network," *IEEE Commun. Mag.*, vol. 58, no. 1, pp. 106–112, Nov. 2020.

[5] Q. Wu and R. Zhang, "Intelligent reflecting surface enhanced wireless network via joint active and passive beamforming," *IEEE Trans. Wireless Commun.*, vol. 18, no. 11, pp. 5394–5409, Nov. 2019.

[6] M. Di Renzo *et al.*, "Reconfigurable intelligent surfaces vs. relaying: Differences, similarities, and performance comparison," *IEEE Open J. Commun. Soc.*, vol. 1, pp. 798–807, 2020.

[7] M. Di Renzo *et al.*, "Smart radio environments empowered by reconfigurable intelligent surfaces: How it works, state of research, and the road ahead," *IEEE J. Sel. Areas Commun.*, vol. 38, no. 11, pp. 2450–2525, Jul. 2020.

[8] S. Zhang, M. Li, M. Jian, Y. Zhao, and F. Gao, "AIRIS: Artificial intelligence enhanced signal processing in reconfigurable intelligent surface communications," *China Commun.*, vol. 18, no. 7, pp. 158–171, Jul. 2021.

[9] Q. Wu and R. Zhang, "Beamforming optimization for wireless network aided by intelligent reflecting surface with discrete phase shifts," *IEEE Trans. Commun.*, vol. 68, no. 3, pp. 1838–1851, May 2020.

[10] M. Cui, G. Zhang, and R. Zhang, "Secure wireless communication via intelligent reflecting surface," *IEEE Wireless Commun. Lett.*, vol. 8, no. 5, pp. 1410–1414, Oct. 2019.

[11] S. Li, B. Duo, X. Yuan, Y.-C. Liang, and M. Di Renzo, "Reconfigurable intelligent surface assisted UAV communication: Joint trajectory design and passive beamforming," *IEEE Wireless Commun. Lett.*, vol. 9, no. 5, pp. 716–720, Jan. 2020.

[12] X. Guan, Q. Wu, and R. Zhang, "Intelligent reflecting surface assisted secrecy communication: Is artificial noise helpful or not?" *IEEE Wireless Commun. Lett.*, vol. 9, no. 6, pp. 778–782, Jun. 2020.

[13] X. Qian *et al.*, "Beamforming through reconfigurable intelligent surfaces in single-user MIMO systems: SNR distribution and scaling laws in the presence of channel fading and phase noise," *IEEE Wireless Commun. Lett.*, vol. 10, no. 1, pp. 77–81, Sep. 2021.

[14] N. S. Perović, L. N. Tran, M. Di Renzo, and M. F. Flanagan, "Achievable rate optimization for MIMO systems with reconfigurable intelligent surfaces," *IEEE Trans. Wireless Commun.*, vol. 20, no. 6, pp. 3865–3882, Jun. 2021.

[15] M. Hua, Q. Wu, D. W. K. Ng, J. Zhao, and L. Yang, "Intelligent reflecting surface-aided joint processing coordinated multipoint transmission," *IEEE Trans. Commun.*, vol. 69, no. 3, pp. 1650–1665, Mar. 2021.

[16] J. Si, Z. Li, J. Cheng, L. Guan, J. Shi, and N. Al-Dhahir, "Covert transmission assisted by intelligent reflecting surface," *IEEE Trans. Commun.*, vol. 69, no. 8, pp. 5394–5408, Aug. 2021.

[17] X. Pang, M. Sheng, N. Zhao, J. Tang, D. Niyato, and K.-K. Wong, "When UAV meets IRS: Expanding air-ground networks via passive reflection," *IEEE Wireless Commun.*, vol. 28, no. 5, pp. 164–170, Oct. 2021.

[18] X. Pang, N. Zhao, J. Tang, C. Wu, D. Niyato, and K.-K. Wong, "IRS-assisted secure UAV transmission via joint trajectory and beamforming design," *IEEE Trans. Commun.*, vol. 70, no. 2, pp. 1140–1152, Feb. 2022.

[19] D. Zhang, Q. Wu, M. Cui, G. Zhang, and D. Niyato, "Throughput maximization for IRS-assisted wireless powered hybrid NOMA and TDMA," *IEEE Wireless Commun. Lett.*, vol. 10, no. 9, pp. 1944–1948, Sep. 2021.

[20] Q. Wu, X. Zhou, W. Chen, J. Li, and X. Zhang, "IRS-aided WPCNs: A new optimization framework for dynamic IRS beamforming," *IEEE Trans. Wireless Commun.*, vol. 21, no. 7, pp. 4725–4739, Jul. 2022.

[21] M. Hua and Q. Wu, "Joint dynamic passive beamforming and resource allocation for IRS-aided full-duplex WPCN," *IEEE Trans. Wireless Commun.*, vol. 21, no. 7, pp. 4829–4843, Jul. 2022.

[22] Z. Li, W. Chen, Q. Wu, H. Cao, K. Wang, and J. Li, "Robust beamforming design and time allocation for IRS-assisted wireless powered communication networks," *IEEE Trans. Commun.*, vol. 70, no. 4, pp. 2838–2852, Apr. 2022.

[23] Q. Wu and R. Zhang, "Weighted sum power maximization for intelligent reflecting surface aided SWIPT," *IEEE Wireless Commun. Lett.*, vol. 9, no. 5, pp. 586–590, May 2020.

[24] Q. Wu and R. Zhang, "Joint active and passive beamforming optimization for intelligent reflecting surface assisted SWIPT under QoS constraints," *IEEE J. Sel. Areas Commun.*, vol. 38, no. 8, pp. 1735–1748, Aug. 2020.

[25] C. Pan *et al.*, "Intelligent reflecting surface aided MIMO broadcasting for simultaneous wireless information and power transfer," *IEEE J. Sel. Areas Commun.*, vol. 38, no. 8, pp. 1719–1734, Aug. 2020.

[26] S. Gong *et al.*, "Beamforming optimization for intelligent reflecting surface-aided SWIPT IoT networks Relying on discrete phase shifts," *IEEE Internet Things J.*, vol. 8, no. 10, pp. 8585–8602, May 2021.

[27] S. Zargari, A. Khalili, Q. Wu, M. R. Mili, and D. W. K. Ng, "Max-min fair energy-efficient beamforming design for intelligent reflecting surface-aided SWIPT systems with non-linear energy harvesting model," *IEEE Trans. Veh. Technol.*, vol. 70, no. 6, pp. 5848–5864, Jun. 2021.

[28] D. Xu, V. Jamali, X. Yu, D. W. K. Ng, and R. Schober, "Optimal resource allocation design for large IRS-assisted SWIPT systems: A scalable optimization framework," *IEEE Trans. Commun.*, vol. 70, no. 2, pp. 1423–1441, Feb. 2022.

[29] Q. Wu, S. Zhang, B. Zheng, C. You, and R. Zhang, "Intelligent reflecting surface-aided wireless communications: A tutorial," *IEEE Trans. Commun.*, vol. 69, no. 5, pp. 3313–3351, May 2021.

[30] R. Long, Y. C. Liang, Y. Pei, and E. G. Larsson, "Active reconfigurable intelligent surface-aided wireless communications," *IEEE Trans. Wireless Commun.*, vol. 20, no. 8, pp. 4962–4975, Aug. 2021.

[31] Z. Zhang *et al.*, "Active RIS vs. passive RIS: Which will prevail in 6G?" 2021, *arXiv:2103.15154*.

[32] N. M. Estakhri and A. Alù, "Wave-front transformation with gradient metasurfaces," *Phys. Rev. X*, vol. 6, no. 4, 2016, Art. no. 041008.

[33] A. Díaz-Rubio, V. S. Asadchy, A. Elsakka, and S. A. Tretyakov, "From the generalized reflection law to the realization of perfect anomalous reflectors," *Sci. Adv.*, vol. 3, no. 8, Aug. 2017, Art. no. e1602714.

[34] M. Di Renzo, F. H. Danufane, and S. Tretyakov, "Communication models for reconfigurable intelligent surfaces: From surface electromagnetics to wireless networks optimization," 2021, *arXiv:2110.00833*.

[35] C. You and R. Zhang, "Wireless communication aided by intelligent reflecting surface: Active or passive?" *IEEE Wireless Commun. Lett.*, vol. 10, no. 12, pp. 2659–2663, Dec. 2021.

[36] K. Liu, Z. Zhang, L. Dai, S. Xu, and F. Yang, "Active reconfigurable intelligent surface: Fully-connected or sub-connected?" *IEEE Commun. Lett.*, vol. 26, no. 1, pp. 167–171, Jan. 2022.

[37] P. Zeng, D. Qiao, Q. Wu, and Y. Wu, "Throughput maximization for active intelligent reflecting surface-aided wireless powered communications," *IEEE Wireless Commun. Lett.*, vol. 11, no. 5, pp. 992–996, May 2022.

[38] G. Chen, Q. Wu, C. He, W. Chen, J. Tang, and S. Jin, "Active IRS aided multiple access for energy-constrained IoT systems," 2022, *arXiv:2201.12565*.

[39] N. Thanh Nguyen, V.-D. Nguyen, Q. Wu, A. Tolli, S. Chatzinotas, and M. Juntti, "Hybrid active-passive reconfigurable intelligent surface-assisted multi-user MISO systems," 2022, *arXiv:2203.07042*.

[40] A. Taha, M. Alrabeiah, and A. Alkhateeb, "Enabling large intelligent surfaces with compressive sensing and deep learning," *IEEE Access*, vol. 9, pp. 44304–44321, 2021.

[41] R. Schroeder, J. He, G. Brante, and M. Juntti, "Two-stage channel estimation for hybrid RIS assisted MIMO systems," *IEEE Trans. Commun.*, vol. 70, no. 7, pp. 4793–4806, Jul. 2022.

[42] G. T. de Araujo and A. L. F. de Almeida, "PARAFAC-based channel estimation for intelligent reflective surface assisted MIMO system," in *Proc. IEEE 11th Sensor Array Multichannel Signal Process. Workshop (SAM)*, Jun. 2020, pp. 1–5.
[43] L. Wei, C. Huang, G. C. Alexandropoulos, C. Yuen, Z. Zhang, and M. Debbah, "Channel estimation for RIS-empowered multi-user MISO wireless communications," *IEEE Trans. Commun.*, vol. 69, no. 6, pp. 4144–4157, Mar. 2021.
[44] K. Meng, Q. Wu, S. Ma, W. Chen, and T. Q. S. Quek, "UAV trajectory and beamforming optimization for integrated periodic sensing and communication," *IEEE Wireless Commun. Lett.*, vol. 11, no. 6, pp. 1211–1215, Jun. 2022.
[45] S. Boyd and L. Vandenberghe, *Convex Optimization*. Cambridge, U.K.: Cambridge Univ. Press, 2004.
[46] Y. Huang and D. P. Palomar, "Rank-constrained separable semidefinite programming with applications to optimal beamforming," *IEEE Trans. Signal Process.*, vol. 58, no. 2, pp. 664–678, Feb. 2010.
[47] I. Pólik and T. Terlaky, *Interior Point Methods for Nonlinear Optimization*. Berlin, Germany: Springer, 2010.
[48] Y. Nesterov and A. Nemirovskii, *Interior-Point Polynomial Algorithms in Convex Programming*. Philadelphia, PA, USA: SIAM, 2004.
[49] Q. Wu and R. Zhang, "Intelligent reflecting surface enhanced wireless network: Joint active and passive beamforming design," in *Proc. IEEE Global Commun. Conf. (GLOBECOM)*, Dec. 2018, pp. 1–6.
[50] D. Xu *et al.*, "Resource allocation for IRS-assisted full-duplex cognitive radio systems," *IEEE Trans. Commun.*, vol. 68, no. 12, pp. 7376–7394, Dec. 2020.

Ying Gao received the B.Eng. degree in electronic information engineering from the Nanjing University of Science and Technology, Nanjing, China, in 2016, and the Ph.D. degree in communications and information systems from the Shanghai Institute of Microsystem and Information Technology, Chinese Academy of Sciences, Shanghai, China, in 2021. She is currently a Post-Doctoral Fellow with the State Key Laboratory of Internet of Things for Smart City, University of Macau. Her current research interests include intelligent reflecting surface (IRS) assisted communications, unmanned aerial vehicle (UAV) enabled communications, physical layer security, and optimization theory.

Qingqing Wu (Senior Member, IEEE) received the B.Eng. degree in electronic engineering from the South China University of Technology in 2012 and the Ph.D. degree in electronic engineering from Shanghai Jiao Tong University (SJTU) in 2016.

From 2016 to 2020, he was a Research Fellow with the Department of Electrical and Computer Engineering, National University of Singapore. He is currently an Assistant Professor with the State Key Laboratory of Internet of Things for Smart City, University of Macau. He has coauthored more than 100 IEEE journal articles with 25 ESI highly cited papers and eight ESI hot papers, which have received more than 13,000 Google citations. His current research interests include intelligent reflecting surface (IRS), unmanned aerial vehicle (UAV) communications, and MIMO transceiver design. He was listed as the Clarivate ESI Highly Cited Researcher in 2021, the Most Influential Scholar Award in AI-2000 by Aminer in 2021, and the World's Top 2% Scientist by Stanford University in 2020 and 2021. He was a recipient of the IEEE Communications Society Young Author Best Paper Award in 2021, the Outstanding Ph.D. Thesis Award of China Institute of Communications in 2017, the Outstanding Ph.D. Thesis Funding in SJTU in 2016, the IEEE ICCC Best Paper Award in 2021, and the IEEE WCSP Best Paper Award in 2015. He is the Workshop Co-Chair for IEEE ICC 2019–2022 Workshop on "Integrating UAVs into 5G and Beyond" and the Workshop Co-Chair for IEEE GLOBECOM 2020 and ICC 2021 Workshop on "Reconfigurable Intelligent Surfaces for Wireless Communication for Beyond 5G." He serves as the Workshops and Symposia Officer for Reconfigurable Intelligent Surfaces Emerging Technology Initiative and a Research Blog Officer for Aerial Communications Emerging Technology Initiative. He is the IEEE Communications Society Young Professional Chair in Asia–Pacific Region. He was an Exemplary Editor of IEEE COMMUNICATIONS LETTERS in 2019 and an exemplary reviewer of several IEEE journals. He serves as an Associate Editor for IEEE TRANSACTIONS ON COMMUNICATIONS, IEEE COMMUNICATIONS LETTERS, IEEE WIRELESS COMMUNICATIONS LETTERS, IEEE OPEN JOURNAL OF THE COMMUNICATIONS SOCIETY, and IEEE OPEN JOURNAL OF VEHICULAR TECHNOLOGY. He is the Lead Guest Editor for IEEE JOURNAL ON SELECTED AREAS IN COMMUNICATIONS on "UAV Communications in 5G and Beyond Networks" and a Guest Editor for IEEE OPEN JOURNAL OF VEHICULAR TECHNOLOGY on "6G Intelligent Communications" and IEEE OPEN JOURNAL OF THE COMMUNICATIONS SOCIETY on "Reconfigurable Intelligent Surface-Based Communications for 6G Wireless Networks."

Guangchi Zhang received the B.S. degree in electronic engineering from Nanjing University, Nanjing, China, in 2004, and the Ph.D. degree in communication engineering from Sun Yat-sen University, Guangzhou, China, in 2009. He has been with the School of Information Engineering, Guangdong University of Technology, Guangzhou, since 2009, and currently a Professor. He was a Senior Research Associate with the City University of Hong Kong from October 2011 to March 2012 and a Visiting Professor with the National University of Singapore from January 2017 to January 2018. His research interests include multiple-input multiple-output, wireless relaying, wireless power transfer, unmanned aerial vehicle enabled communications, intelligent reflecting surface assisted communications, physical layer security, and artificial intelligence enabled communications. He was a recipient of the IEEE Communications Society 2014 Heinrich Hertz Award and the IEEE COMMUNICATIONS LETTERS 2014 Exemplary Reviewer.

Wen Chen (Senior Member, IEEE) is currently a Professor (tenured) with the Department of Electronic Engineering, Shanghai Jiao Tong University, China, where he is the Director of the Broadband Access Network Laboratory. He has published more than 110 articles in IEEE journals and more than 120 papers in IEEE conferences, with citations more than 8000 in Google Scholar. His research interests include multiple access, wireless AI, and meta-surface communications. He is a fellow of the Chinese Institute of Electronics. He is the Shanghai Chapter Chair of IEEE Vehicular Technology Society. He is an Editor of IEEE TRANSACTIONS ON WIRELESS COMMUNICATIONS, IEEE TRANSACTIONS ON COMMUNICATIONS, IEEE ACCESS, and IEEE OPEN JOURNAL OF VEHICULAR TECHNOLOGY. He is the Distinguished Lecturer of IEEE Communications Society and IEEE Vehicular Technology Society.

Derrick Wing Kwan Ng (Fellow, IEEE) received the bachelor's (Hons.) and Master of Philosophy (M.Phil.) degrees in electronic engineering from The Hong Kong University of Science and Technology (HKUST) in 2006 and 2008, respectively, and the Ph.D. degree from The University of British Columbia (UBC) in November 2012.

He was a Senior Post-Doctoral Fellow at the Institute for Digital Communications, Friedrich-Alexander-University Erlangen-Nürnberg (FAU), Germany. He is currently working as a Scientia Associate Professor at the University of New South Wales, Sydney, Australia. His research interests include global optimization, physical layer security, IRS-assisted communication, UAV-assisted communication, wireless information and power transfer, and green (energy-efficient) wireless communications. He has been listed as a Highly Cited Researcher by Clarivate Analytics (Web of Science) since 2018. He has received the Australian Research Council (ARC) Discovery Early Career Researcher Award 2017, the IEEE Communications Society Stephen O. Rice Prize 2022, and the Best Paper Awards at the WCSP 2020 and 2021, the IEEE TCGCC Best Journal Paper Award 2018, INISCOM 2018, IEEE International Conference on Communications (ICC) 2018 and 2021, IEEE International Conference on Computing, Networking and Communications (ICNC) 2016, IEEE Wireless Communications and Networking Conference (WCNC) 2012, the IEEE Global Telecommunication Conference (GLOBECOM) 2011 and 2021, and the IEEE Third International Conference on Communications and Networking in China 2008. He has served as an Editorial Assistant to the Editor-in-Chief of the IEEE TRANSACTIONS ON COMMUNICATIONS from January 2012 to December 2019. He is serving as an Editor for the IEEE TRANSACTIONS ON COMMUNICATIONS and the IEEE TRANSACTIONS ON WIRELESS COMMUNICATIONS. He is serving as the Associate Editor-in-Chief for the IEEE OPEN JOURNAL OF THE COMMUNICATIONS SOCIETY.

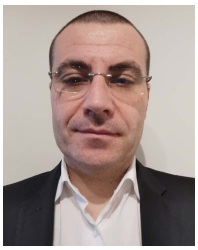

Marco Di Renzo (Fellow, IEEE) received the Laurea *(cum laude)* and Ph.D. degrees in electrical engineering from the University of L'Aquila, Italy, in 2003 and 2007, respectively, and the Habilitation à Diriger des Recherches (Doctor of Science) degree from University Paris-Sud (now Paris-Saclay University), France, in 2013.

He is currently the CNRS Research Director (a Professor) with the Laboratory of Signals and Systems (L2S), Paris-Saclay University—CNRS and CentraleSupelec, Paris, France. He serves as the Coordinator for the communications and networks research area of the Laboratory of Excellence DigiCosme, Paris-Saclay University; a member for the Admission and Evaluation Committee, Ph.D. School on Information and Communication Technologies, Paris-Saclay University; and the Head of the Laboratory of Signals and Systems, Intelligent Physical Communications Group, CentraleSupelec. He is a Founding Member and the Vice Chair of the Industry Specification Group (ISG) on Reconfigurable Intelligent Surfaces (RIS) within the European Telecommunications Standards Institute (ETSI) and the Rapporteur of the work item on communication models, channel models, and evaluation methodologies. He is a fellow of IET and AAIA. He is an Ordinary Member of the European Academy of Sciences and Arts and the Academia Europaea. He is a Highly Cited Researcher. He is also a Fulbright Fellow and was a Nokia Foundation Visiting Professor and a Royal Academy of Engineering Distinguished Visiting Fellow. His recent research awards include the 2021 EURASIP Best Paper Award, the 2022 IEEE COMSOC Outstanding Paper Award, and the 2022 Michel Monpetit Prize from the French Academy of Sciences. He serves as the Editor-in-Chief for IEEE COMMUNICATIONS LETTERS.